Stony Brook University

Biophysical properties of Cx40 mutants as they relate to Atrial Fibrillation

A Dissertation Presented

by

Ana Santa Cruz

to

The Graduate School

in Partial Fulfillment of the

Requirements

for the Degree of

Doctor of Philosophy

in

Physiology and Biophysics

Stony Brook University

May 2015

Stony Brook University

The Graduate School

Ana Santa Cruz

We, the dissertation committee for the above candidate for the

Doctor of Philosophy degree, hereby recommend

acceptance of this dissertation.

Dr. V. Valiunas – Dissertation Advisor
Research Associate Professor,
Physiology and Biophysics Department

Dr. Thomas W. White - Chairperson of Defense
Professor,
Physiology and Biophysics Department

Dr. Peter R. Brink
Professor and Chairman
Physiology and Biophysics Department

Dr. Raafat El-Maghrabi
Research Associate Professor
Physiology and Biophysics Department

Dr. Vytautas K. Verselis
Professor of Neuroscience
Albert Einstein College of Medicine

This dissertation is accepted by the Graduate School

Charles Taber
Dean of the Graduate School

Abstract of the Dissertation

Biophysical properties of Cx40 mutants as they relate to Atrial Fibrillation

by

Ana Santa Cruz

Doctor of Philosophy

in

Physiology and Biophysics

Stony Brook University

2015

Gap junctions (GJs) are integral membrane proteins and are the only known cellular structures that allow a direct cell-to-cell transfer of signaling molecules by forming densely packed arrays of hydrophilic channels that bridge the opposing membranes of neighboring cells. A gap junction channels is formed with two hexameric connexons. Each connexon is comprised of six connexin subunits. Cell-to-cell action potential propagation in the heart is mediated through gap junction channels that are located in regions called intercalated discs found at lateral cell to cell borders in cardiomyocytes. The three Cx40 mutations (A96S, M163V and G38D) are associated with atrial fibrillation and retain the ability to form functional channels. This dissertation is motivated by questions such as how these mutations could be changing the biophysical and expression properties of the channels compared to wild type (WT) Cx40. In our first aim, we showed that all three mutations exhibited a similar macroscopic coupling and also similar voltage dependencies comparable to WT Cx40. We also showed that the unitary conductance of G38D channels was higher than the WT Cx40. The A96S and M163V mutants exhibited unitary conductances comparable to the WT. In the second aim, we showed that the M163 and G38D mutations exhibited a higher LY (Lucifer yellow) permeability when compared with WT, while the A96S permeability is very similar to WT. A96S and M163V exhibited a higher EthBr (Ethidium bromide) permeability when compared with wild type and G38D is almost impermeable. Finally in our third aim, we showed that all the mutants are able to reach the membrane and form plaques. The results of our work show that even when the three mutations exhibited a similar total conductance and voltage dependence the permeability of the mutations to LY and EthBr is different when compared with WT. An important role of Cx is their ability to form intracellular channels capable of supporting intercellular exchange of

molecules up to 1,000 Da. The change in permeability properties of the mutations could be implicated in the mechanism of atrial fibrillation and reentry arrhythmias.

A mi mama.

> “He allowed himself to be swayed by his conviction that human beings are not born once and for all on the day their mothers give birth to them, but that life obliges them over and over again to give birth to themselves.” -- "Love in the Time of Cholera". GGM

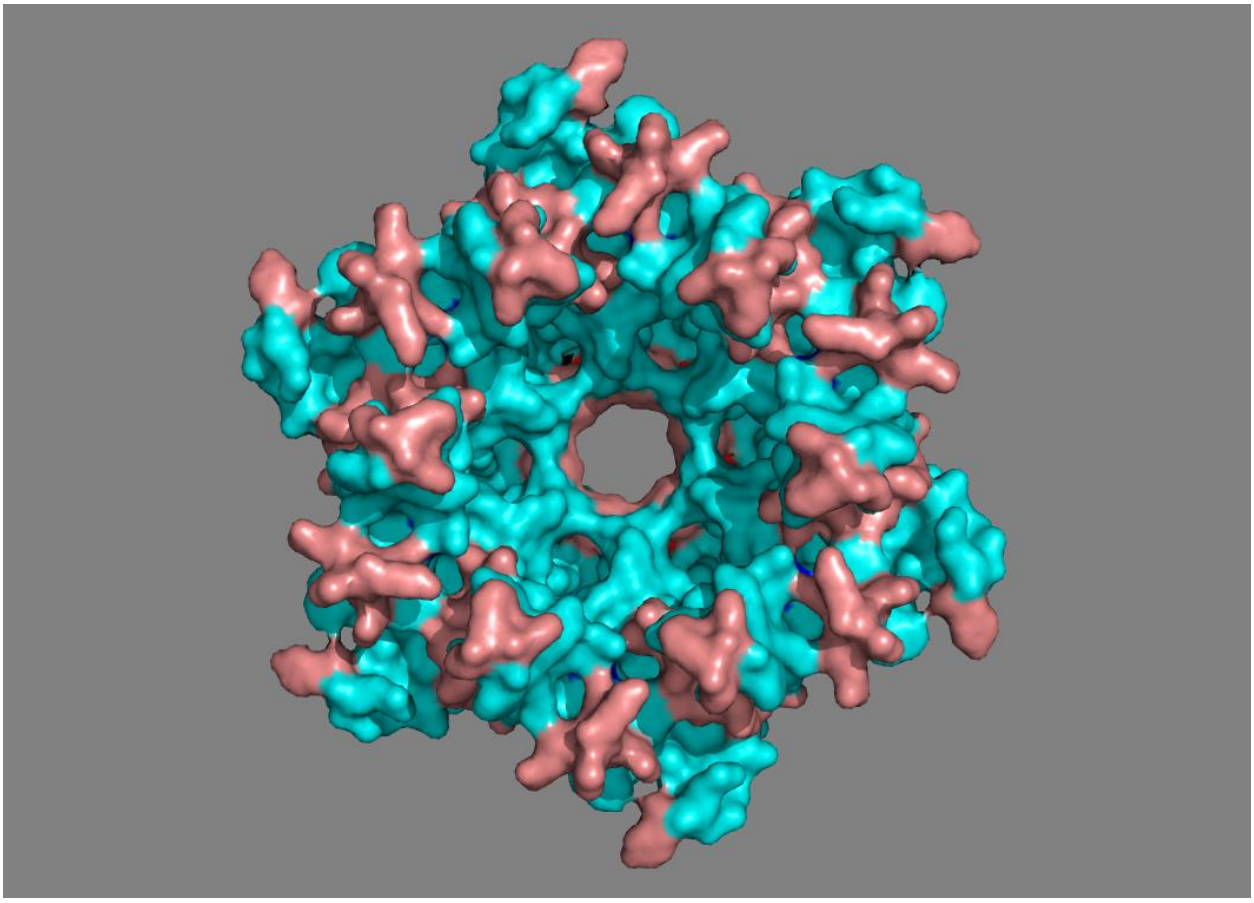

Table of Contents

List of Figures/Tables/Illustrations

List of Abbreviations

AF – Atrial fibrillation

AGJ – Annular gap junctions

ATP – Adenosine triphosphate

AV – Atrioventricular bundle

AVN – Atrioventricular node

Ca2+ - Calcium ion

cAMP – Cyclic adenosine monophosphate

cGMP – Cyclic guanosine monophosphate

CL – Cytoplasmic domain

CT – C-Teminal

CV – Conduction velocity

Cx – Connexin

Cx26 – Connexin 26

Cx40 – Connexin 40

Cx43 – Connexin 43

Cx45 – Connexin 45

DAD – Delayed afterdepolarization

EAD – Early afterdepolarization

EC – Extracellular domain

ER – Endoplasmic reticulum

ERAD - ER-associated degradation

ERGIC - ER-Golgi intermediate compartment

GJ – Gap junction

gj – Total conduction of the junction

GJIC – GJ-mediated intercellular communication

ID – Intercalated disc

IL – Intracellular loop

IP3 – inositol trisphosphate

K+ - Potassium ion

N – Total number of channels

Na+ - Sodium ion

mV – mini volts

NT – N-Terminal

Panx – Pannexin

Po – Open probability

pS – pico siemens

SACM – Substituted cysteine accessibility method

SAN – Sinoatrial node

TM – Transmembrane domain

Vj – Junctional voltage

WT – Wild type

Acknowledgments

This dissertation would not have been possible without the help of so many people in so many ways:

First I would like to thank my advisor Dr. Valiunas. Thank you for teaching me to think for myself, and for all your understanding, guidance and advice. He is an excellent patch-clamper and I am so thankful for the opportunity to learn from one of the best.

I should especially like to give thanks to Dr. Brink for all his assistance and guidance in my work and in my life. I wouldn't be where I am without him. He is one of the smartest people I know. He has led me to aspire to great things.

I must also thank the members of Dr. Brink's lab. Chris Gordon and Dr. Wang are some of the most talented, helpful and amazing people I've ever met. All of their help, support, and understating were invaluable. They don't have an idea of how a simple smile from them in the morning could change my entire day.

I would like to thank Laima for all her help. Without her hard work I wouldn't be able to do my research. Thank you so much for all your hard work.

I would like to express my appreciation to my committee, Dr. Thomas White, Dr. Raafat El-Maghrabi and Dr. Vytautas Verselis, for all their help and assistance during all this process.

I would like to give a special thanks to Dr. El-Maghrabi for his understanding and support. for all his help, support and assistance. Without his help all of this wouldn't be possible.

I would like to acknowledge the Physiology and Biophysics Department. Everyone is very helpful and friendly, and always able to answer a question or give some advice. They all helped me to develop my knowledge in physiology. I want to give a special thank you to Odalis Hernandez for all of her assistance with papers, due dates, and the elimination of all my administrative problems. I would like to thank Melanie, who unfortunately is not with us anymore, for all her help when I first arrived in this country. She made my transition very easy and helped me a lot. Thank to Joan Kavanaugh, department administrator and Michele Leva for all their help.

I would like to thank Dr. Dilger, who was always willing to help and give me his best suggestions.

Finally I want to thank my family. I specifically want to thank my mum. She is the most amazing mother ever, she was the one who has raised me, support me and always always be for me. She is the most important person in my life. All my family down in Mexico thanks for all your cheers

and support. I also want to thank Jamie (best boyfriend in the universe ever). He is the one dealing with my craziness every day. He makes me laugh, he keeps me safe and he buys a squirrel poo milkshake every time that I had a bad day!!!. He just keeps me sane and happy.

Chapter 1

Introduction

Gap Junctions

In all multicellular organisms, the cells of almost all tissues are connected to each other by specialized intracellular channels called gap junctions (GJ). These channels are critical for the development and function of these tissues. GJ are composed of integral membrane proteins that connect the cytoplasm of neighboring cells (Nielsen et al., 2012), providing both metabolic and electrical coupling (van Veen et al., 2001). The metabolic coupling allows the passage of small molecules up to ~1,000 daltons in size (Nielsen et al., 2012) including secondary messengers, small metabolites, and ions. The transfer of larger solutes, fluorescently labelled oligonucleotides (morpholinos) up to 24 nucleotides in length through Cx43 has been reported (Valiunas et al., 2005). The electrical coupling is essential for the propagation of the electrical signals from cell-to-cell. GJ are formed by three different classes of proteins, innexins, pannexins and connexins (Fig.1). The GJ in invertebrates are formed by innexins (Phelan, 2005). In vertebrates the GJ are formed by connexins. The third group of GJ, pannexins, were described for the first time in 2000 in the mammalian genome (Panchin et al., 2000).

-Innexins

In invertebrates, cell-to-cell communication occurs via GJ proteins called innexins (Inx) (Phelan et al., 1998). Inx proteins are predicted to have four transmembrane domains, one intracellular and two extracellular loops, and cytoplasmic C- and N-terminal tails (Barnes, 1994). Inx

associate to form hexameric pore structures (known as "innexons") that loosely aggregate at points of cell-to-cell contact (Oshima et al., 2013). This may allow them to behave in an analogous fashion to connexins, with a hexamer from one cell "docking" with another on the adjacent cell, thus forming an intercellular GJ (Phelan et al., 1998a). Innexons can be composed of a single isotype ("homomeric") or multiple isotypes ("heteromeric") (Stebbings et al., 2000), and docking between innexons can be "homotypic" or "heterotypic," depending on whether each half is constructed from the same isotype or not (Wu et al., 2011). Inx have been shown to form functional intracellular channels that are voltage and pH sensitive (Landesman et al., 1999).

-Pannexins

Panchin et al., in 2000 performed a screen to uncover homologues of the Inx family in the mammalian genome. The investigation resulted in the identification of a second family of proposed GJ proteins in vertebrates, pannexins (Panx). Panx exhibit a topology analogous to connexins and Inx, four alpha-helical transmembrane (TM) domains connected by two extracellular (EC) loops and a single cytoplasmic loop; both N- and C- terminals are intracellular (Herve and Denangeron, 2013) (Fig.1). These proteins form single-membrane channels that are regulated by post-translational modifications, channel intermixing and sub-cellular expression profiles (Penuela et al., 2013). Panxs form large gated pores between the intracellular and extracellular space, in a way that is reminiscent of connexin hemichannels (Bond and Naus, 2014). Some research has showed that under certain circumstances, Panx-based intercellular channels will form. For example, over-expression in Xenopus paired oocytes reveals appreciable levels of transjunctional current attributable to Panx1 or co-expressed Panx1/2 (Bruzzone et al., 2003). Even when the channels could be paired and exhibit transjunctional current, it takes

upwards of 24 h for these channels to accumulate, and the macroscopic currents are weak compared to connexin-based GJ (Boassa et al., 2007).

-Connexins

Connexin Structure

In mammals GJs are composed of proteins called connexins. Cx GJs are formed of two hemichannels or connexons from different cells that dock to form a complete GJ. Each hemichannel is formed by six Cx (Fig.2). There are 21 different Cx genes in humans and 20 in mice. Cx genes are classified according to sequence homology and are divided into five subfamilies: α (GJA), β (GJB), γ (GJC), δ (GJD) and ε (GJE) (Cruciani and Mikalsen, 2006). The most widely used nomenclature system uses the word connexin abbreviated as Cx, followed by a suffix indicating the molecular weight in kilodaltons i.e. Cx40= 40kDa. The connexons are homomeric when they contain only one Cx type or heteromeric when they contain different Cx. When the GJ is formed by two identical connexons they are named homotypic channels; and when the channel is formed by two different connexons they are named heterotypic channels (Fig.3).

The Cx channel topology consists of four membrane-spanning segments (TM1-TM4), with the C-terminal (CT) and N-terminal (NT) domains toward the intracellular side. Three loops connect the TM segments, one cytoplasmic (CL), and two extracellular (E1 and E2) (Fig4.). The TM domains and the extracellular loops display the highest conservation in sequence (Beyer et al., 1987) and the most variable domains are the CT and the CL connecting TM2 to TM3.

In hemichannels, residues in TM1 and the EC1 (Kronengold et al., 2003), as well as TM3 (Zhou et al., 1999) have been identified as lining the channel. It has been proposed that the pore of the channel is lined by amino acids from the TM2 and TM3 domains (Skerrett et al., 2002), it has been also proposed that parts of the CL also are lining the pore.

Skerrett et al. in 2002 using SCAM (substituted cysteine accessibility method) proposed that TM2 and TM3 are the pore lining domains for open GJ channels composed of Cx32. In the same paper they concluded that the TM3 is the major pore lining segment of the GJ channel. Skerrett et al., results are similar to the major pore lining helix in the model proposed by Unger in 1999. In 2004 Fleishman et al., predicted the location of α-carbons for the amino acids within the TM helices, and assigned specific helices based on evolutionary conservation of amino acids, distribution of disease related mutations, and effects of site directed mutagenesis. This model proposes that the TM3 forms the majority of the channel pore and TM1 also could be lining the pore. In 2003 Kroenengold et al., demonstrated that residues in the EC1 of Cx46, near the EC1-TM1 border, to be pore-lining. Two of the identified residues in EC1 are negatively charged and likely constitute the locus of fixed negative charge previously indicated by domain substitution. Continued accessibility of residues in TM1 indicates that the pore continues from EC1 to TM1 as it enters the TM span. Using computer simulation Pantano et al., in 2008 provided a model for different TM domains. In this model TM3 formed the majority of the pore with contribution of the EC2.

In 2009, Maeda et al., published the structure of Cx26 at 3.5 Å resolution. They concluded that the TM1 and TM2 are facing the luminal side of the pore, but because TM2 and part of the TM1 (cytoplasmic part) are covered by NT, the TM2 and part of TM1 are not really exposed to the

lumen. TM3 and TM4 are facing the lipid. Maeda et al. data support the model proposed by Kronengold et al., in which TM1 is the major helix lining the pore.

The extracellular domains of all Cxs contain three cysteine residues located in each of the CL (Dahl et al., 1992), E1 and E2 mediate the docking of hemichannels, and it is possible that EC2 contains the determinants for heterotypic interactions (Haubrich et al., 1996).

In 2012, Kronengold et al., using SCAM and chimeric data, reported that the NT, TM1 and E1 domains are the core elements that constitute the Cx pore as well as the essential components necessary for voltage-dependent gating.

Connexin Formation and Degradation

Cxs are generally considered to be co-translationally inserted into the endoplasmic reticulum (ER) (Leithe et al., 2012) (Fig.5). The location at which Cxs oligomerize into connexons is Cx-type dependent (Das Sarma et al., 2002). Cx32 appears to assemble in the ER but Cx43 assembles in the Golgi. Upon exiting the ER, properly folded Cx are expected to pass through the ER-Golgi intermediate compartment (ERGIC) prior to entering the cis-Golgi network (Laird D.W., 2006) (Fig.5). The general consensus emerging is that trafficking the Cxs to the plasma membrane first requires their rapid oligomerisation into connexons (Koval M, 2002). Trafficking of connexons from the Golgi to the plasma membrane depends on an intact cytoskeleton (Nielsen et al., 2014).

After oligomerization, connexons are transported to the plasma membrane via the vesicular transport mechanism (Fig.5). Connexons can be inserted into the plasma membrane either

directly into the plaque region (Guerrier et al., 1995), or randomly in the membrane and then translocated laterally into the plaque region (Johnson et al., 1974). GJ plaques are clusters of GJ channel arranged into two dimensional sheets. These plaques can extend from several nanometers to several micrometers in diameter (McNutt and Weinstein, 1970).

Cxs have a short half-life, 1-5 h (Berthoud et al., 2004). GJ plaques are internalized from the plasma membrane in vesicle-like double membrane structures named annular gap junctions (Fig.5). This process is generated by the invagination, restriction, pinching-off and transport of both junctional membranes into the cytoplasm of one of the apposed cells for further degradation (Segratain and Falk, 2004). The degradation of the GJ proceeds via one of two pathways; the proteasomal or the lysosomal degradation pathways.

The proteasome is a 26S holoenzyme complex comprised of 2 major subunits, the 20S core and the 19S cap or regulatory particles which are each made up of multiple individual protein subunits (Voges et al., 1999). ER-associated degradation (ERAD) is the process responsible for the removal and proteasomal degradation of misfolded proteins localized to the ER. During ERAD, misfolded proteins in the ER are recognized by a molecular chaperone such as Bip, transported out of the ER through the retrotranslocon channel into the cytoplasm to be degraded by the proteasome (Su and Lau, 2012).

The lysosomal pathway consist of two separate routes, the endo-/lysosomal and the phago-/lysosomal (termed macroautophagy). The endo-/lysosomal pathway is designed for the uptake of extracellular nutrients and factors via the formation and internalization of vesicles from the plasma membrane. These vesicles then fuse with endosomes and lysosomes to degrade the cargo (Falk et al., 2014). The macroautophagy is the lysosomal pathway responsible for the

degradation of structures already located in the cytoplasm. The preference for one degradative pathway over the other may be cell type dependent and within the same cell type the degradative pathway chosen might depend on the metabolic state of the cell.

Connexins Physiological function

GJ channels are essential for the maintenance of tissue function and homeostasis. Cxs could also be active as functional hemichannels in nonjunctional membranes linking the cytoplasm of the cell with the extracellular environment. The GJ are also fundamental for the cell-to-cell transfer of current or electrical coupling of the cells in excitable tissue, like the heart. They also are essential for the exchange of larger molecules in both excitable and non-excitable tissues (Valiunas et al., 2002).

Cardiac Gap Junctions

Cardiac Morphology and Function

The heart is a powerful muscle that functions as the body's circulatory pump. It takes in deoxygenated blood through the veins and delivers it to the lungs for oxygenation before pumping it into the various arteries, providing oxygen and nutrients to body tissues by transporting the blood throughout the body and removing metabolic products by repeated rhythmic contractions. Under normal physiological conditions the heart contracts steadily and uninterruptedly, changing its rate according to changes in systemic needs. A normal human heart performs an average of 100,000 coordinated contractions every day (Schmitt et al., 2014).

The heart is made up of 4 chambers, 2 atria and 2 ventricles. De-oxygenated blood returns to the right side of the heart via the venous circulation. It is pumped from the right atria into the right ventricle and then to the lungs where carbon dioxide is released and oxygen is absorbed. The oxygenated blood then travels back to the left side of the heart into the left atria, then into the left ventricle from where it is pumped into the aorta and arterial circulation.

The wall of the heart is composed of three layers: the outermost epicardium, the middle myocardium, and the inner endocardium. The myocardium is the thick contractile middle layer of uniquely constructed and arranged muscle cells that forms the bulk mass of the heart wall containing a minimum of other tissue, except of blood vessels. The myocardium is capable of organized contraction and relaxation propelling blood through the arteries. The myocardium consists of a three-dimensional arrangement of rod-shaped cardiomyocytes attached to adjacent myocytes to form myofibers (Bird et al., 2003). These cells are striated, although the pattern is not as ordered as in skeletal muscle. The region where one cardiomyocyte abuts another is called an intercalated disc (ID), a specialized intercellular junctional structure found only in cardiac tissue (Li J, 2014). The original description of the ID identified three structures, adherens junctions, desmosomes, and GJ. GJ form dynamic inter-cellular aqueous pores or channels from Cxs (Severs et al., 2008).

Contraction of the heart occurs when the myocardium is excited by action potentials that propagate through the heart conduction system. The conduction system is composed of specially modified fibers of myocardial muscle and include the sinoatrial node (SAN), the atrioventricular node (AVN), the atrioventricular (AV) bundle and the Purkinje fibers. The action potential triggers an intracellular signal pathway known as excitation-contraction coupling (Olesen et al., 2014).

In the heart, GJs mediate electrical coupling between cardiac myocytes, forming the cell-to-cell pathways for orderly spread of the wave of electrical excitation responsible for synchronous contraction. Thus, the heart is a functional syncytium. The normal heart rhythm depends fundamentally on this coupling of cardiac myocytes by GJ (Servers et al., 2008).

Cardiac Action Potential

An action potential is an electrical stimulation created by a sequence of ion fluxes through specialized channels in the membrane of cardiomyocytes that leads to cardiac contraction. The cardiac action potential consists of five phases, beginning and ending with phase 4. The different phases are:

(Fig.6)

-Phase 4.- Is the interval between full repolarization and the initiation of the next action potential. The cardiac myocytes are at resting membrane potential around - 90 mV in normal working myocardial cells (Grant AO, 2009) due to a constant leak of K+ through inward rectifier channels. Na+ and Ca2+ channels are closed. In the standard myocyte model this phase will be a horizontal line (Sherwood L., 2008).

- Phase 0.- Is the phase of rapid depolarization. An action potential triggered in a neighbouting cardiomyocyte or pacemaker cell causes the membrane potential shifts into a positive voltage range and it peaks at about +25 mV inside the cell. This abrupt shift in the membrane potential is driven by the influx of Na, INa< through the voltage gated Nav1.5 channel. L-type (long-

opening) Ca2+ channels open when the membrane potential is greater than -40 mV and cause a small but steady influx of Ca2+ down its concentration gradient. This phase is crucial for the rapid propagation of the cardiac impulse (conduction velocity ɵ= 1m/s) (Grant AO, 2009). The slope of this phase represents the maximum rate of potential change. in heart muscle cells, this slope is directly proportional to the net ionic current (Carmeliet and Vereecke, 2002).In heart pacemaker cells, this phase depends on the activation of L-type calcium channels instead of the fast Na+ current. The action potentials in autorhythmic cells are caused by the large influx of calcium ions not sodium ions like in contractile cells (Sherwood, 2012).

- Phase 1.- Is the rapid repolarization component of the action potential. This phase is due to almost total inactivation of INa and ICa2+ (Grant AO , 2009) and the activation of transient voltage-gated K+ currents (Ito).

- Phase 2.- Is the plateau phase, and is the longest phase. This long depolarized plateau is a pre-requisite for excitation-contraction coupling and is caused by a balance between outward K+ currents and inward currents through voltage gated Ca2+ channels. These two currents are electrically balanced and the membrane potential is maintained at a plateau just below 0 mV throughout phase 2.

- Phase 3.- Is the phase of rapid repolarization that restores the membrane potential to its resting value (Grant AO, 2009). The repolarization is caused by the balance between inactivating Ca2+ current and rising K+ channels tilting quickly towards later (Schmitt et al., 2014). Normal transmembrane ionic concentration gradients are restores by returning Na+ and Ca2+ ions to the extracellular environment, and K+ ions to the cell interior.

Under physiological conditions, a given cardiomyocyte in the adult working myocardium is electrically coupled to an average of 11 adjacent cells in the ventricle and around 6-7 cells in the crista terminalis (Saffitz et al., 1995) with GJ being predominantly localized at the ID at the ends of the rod shaped cells (Saffitz et al., 1994). While most of the GJ are found at the ends of the cardiomyocytes, some are found in the transverse direction (or sides) (Kanno and Saffitz, 2011). As a consequence electrical conduction in the longitudinal direction, along axis of the fibers, is much greater than that in the transverse direction, perpendicular to the fiber direction (Saffitz et al., 1994). This implies that the electrical conduction within the heart is anisotropic; that the electrical properties of the cardiac tissue vary in different directions, depending on the orientation of the fibers. The structural determinants of anisotropic conduction are cell geometry, cell size and directional distribution of GJ and membrane channels (Valderrabano M., 2007). The cardiac tissue has a faster conduction velocity (CV) along fiber direction than across it, a property implicated in arrhytmogenesis (de Diego et al., 2011). Gap junctional conductance determines the intracellular resistivity, which modulate CV and is greater in the transverse direction than in the longuitudinal direction, a phenomenon related to GJ plaque size and Cx density (Kanno and Saffitz, 2011). The crista terminalis of the right atrium is an example of this anisotropy, where the ratio of longitudinal to transverse CV is approximately 10:1 (Saffitz et al., 1995). CV propagation is uniform in multicellular tissue under normal conditions and is continuous (Rohr S, 2004). During GJ uncoupling or a severe conductance reduction, the CV is not only drastically reduced but will also result in a meandering activation wave which have been associated with atrial fibrillation (Ikeda et al., 1997). A simple meandering functional reentrant wave could result in rapid and irregular electrical activity, leading to arrhythmia (Gray et al., 1995). Meandering is induced by the presence of islands of completely uncoupled cells,

which causes the activation wave to follow a "zig-zag" path instead of a continuous propagation (Rohr S, 2011). The GJ coupling is crucial for impulse propagation in cardiac tissue. A reduction of the junctional conductance is an important contributor to arrhytmogenesis because a reduction in the junctional conductance results in a reduction of CV.

Connexin Expression in the Heart

The role of GJ-mediated intercellular communication (GJIC) is crucial for all aspects of multicellular life, including coordination of development, tissue function and cell homeostasis (Thevenin et al., 2013). Cell-to-cell action potential propagation in the heart is mediated through GJ channels that are located in regions called intercalated discs found at lateral cell-to-cell borders in cardiomyocytes providing an end-to-end cell coupling. The three major types of connexin in the heart are Cx40, Cx43 and Cx45 (Gros et al., 1996), with Cx43 expressed at much higher levels compared to the other two Cx (Van-Kempen et al., 1996). Different regions of the heart show specific profiles of Cx expression (Fig.7). Differences in abundance, size and locations in different cardiac regions may contribute to differences in their properties of electrical conduction.

Connexin 40 : Cx 40 is one of the two major atrial Cx, Cx43 being the other one. Cx40 also is expressed in the ventricular conduction system with Cx45 (Veenstra et al., 1992) and in very low levels in the SAN (sino atrial node) and AVN (atrio ventricular node) (Kwong et al., 1998). Cx40 channels are mildly sensitive to the transjunctional voltage (Vj) with a half maximal inactivation at +/-50 mV (Beblo et al., 1995). The unitary conductance is between 120-220 pS, depending on the paper, for example, Cottrell at al.,2002 reported a range from 155-220 pS.,

Valiunas et al., 2002, reported 125 pS., Traub et al., 1994 reported 121 pS., Beblo et al., 1995 reported 158 pS., Bakauskas et al., 1995 reported 198 pS., and Hellmann et al., 1996 reported 175 pS. Cx40 is also regulated by internal pH (Peracchia C., 2004). Cx40 allows the passage of both cationic and anionic dyes but presents more permeability for negatively charged probes like Lucifer Yellow than for positively charged probes like ethidium bromide (Kanaporis et al., 2011). Cx40 is found in both a phosphorylated and non-phosphorylated configuration (Delorme et al., 1995), and the human Cx40 protein contains seven putative sites for phosphorylation by protein kinase C.

Connexin 43: Cx43 is the main Cx in the heart. It is expressed in the atria, ventricles and conduction system, except in the SAN and AVN (Davis et al., 1995). Cx43 is not very sensitive to the Vj, with a half maximal inactivation at +/-40 mV. Cx43 has a very high permeability for negative charge molecules and less permeability for positive ones (Kanaporis et al., 2011). Cx43 is a known phospho-protein and its amino acid sequence contains putative phosphorylation consensus sequences for PKC, PKA, PKG and MAP kinases in its carboxy-terminus (Kemp and Pearson, 1990).

Connexin 45: Cx45 is expressed mainly in the ventricular conduction system , in the SAN and AVN and it is also expressed at very low levels in the atria and ventricles. Cx45 is highly sensitive to Vj, with a half maximal inactivation at +/-20 mV (Moreno et al., 1995). Unitary conductance is around 20-40 pS depending on the source, for example Elenes et al., 2001 reported 38 pS., van Veen et al., 2000 reported 21 and 38 pS and Bakauskas et al., 2002 reported 32 pS. It is permeable to negatively charged molecules (less than Cx43 but more than Cx40) and is almost impermeable to positively charged probes in compared with Cx43 and Cx40 (Kanaporis et al., 2011). It contains phosphorylation sites for PKC, PKA and PKG.

Gap Junction Mutations in Cardiac Disease

GJ mediate the cell-to-cell propagation of the very precisely and organized patterns of current flow that govern orderly contraction of the healthy heart (Severs *et al.,* 2004). Alterations in GJ number, cellular distribution, function and mutations in Cx genes are known to result in different types of cardiac disease like sudden cardiac death and arrhythmias.

The first studies to investigate the role of GJ in atrial fibrillation (AF) were done in animal models. Cx40 knock-out mice studies showed a slow action potential propagation velocity (Kirchhoff *et al.,* 1998, Hagendorff *et al,* 1999 and Verhuele *et al.,* 1999, all reported a slow in the action potential velocity) and an increased vulnerability to induced arrhythmias in the atria. Reduction in Cx40 expression was detected in a model of pacing induced arrhythmias in goats (Van der Velden et al., 2000). Different groups have been investigating the Cx40 expression and distribution in humans during atrial fibrillation. Some studies show an increase in the protein expression of Cx40 and a heterogeneous distribution during AF (Dupont et al., 2001), while other groups report a decrease in the Cx40 protein with a homogenous distribution during the atrial fibrillation (Wilhelm et al., 2006). In 2003 Groenewegen et al. connected the Cx40 gene with AF in humans, this was the first report linking a mutation in Cx40 gene with AF.

Atrial fibrillation is the most common sustained cardiac arrhythmia and one of the most common cardiovascular conditions (Ball et al., 2013). AF is well recognized as a major risk factor for ischemic stroke and transient ischemic attacks (Andrew et al., 2013). Numerous papers have been published describing different cardiac ion channels mutations related with AF including abnormalities in Cx40.

In 2006 Gollob et al. described four mutations in Cx40 that are associated with atrial fibrillation: G38D, P88S, A96S and M163V (Fig.8). The mutations G38D, A96S and M163V form functional channels but the P88S mutation channels are non-functional or the conductance is minimal. Gollob et al., in 2006 also showed that the localization of the Cx40 mutants expressed in N2A cells (neuroblastoma cells) is different from N2A cells expressing the wild type Cx40 (WT). WT Cx40 was localized at the sites of cell-to-cell contact while the P88S mutant doesn't form visible plaques (likely the reason why the N2A cells containing P88S mutant were not electrically coupled). The Cx40 G38D mutant formed very sparse plaques and had high intracellular retention. The Cx40 A96S mutant formed a similar number of plaques as WT, but it was also retained intracellularly. The M163V mutant showed very similar plaque formation and localization as Cx40 WT. Lubkemeier et al., in 2011 describes that the A96S mutation expressed in mice exhibit a renin dependent hypertension. In 2013 Lubkemeier et al., also reported that the A96S mutation caused a decrease in the atrial conduction velocities and sustained episodes of induced AF in mice. They showed that A96S has a low conductance due to an enhanced Vj-gating and reduced channel open probability, while the single channel conductance was similar to that of WT (Lubkemeier et al., 2013).

Yang et al., in 2010 identified three heterozygous missense mutations in 3 of 218 unrelated Chinese families. These mutations are V85I, L221I and L229M (Fig.8). In each family the mutation is present in all the affected members alive but is absent in unaffected members (Yang et al., 2010). Using cross-species evolutionary alignment of Cx40, they showed that that the altered amino acids are completely conserved, suggesting a possible functional relevance. This group also predicted that all the mutations are in amino acids within or near the TM-spanning regions, V85I and L221I are possibly located within the TM2 and TM4 and L229M at the

cytoplasmic region close to the CT (Yang et al., 2010). This group also suggests that the three mutations could perturb cardiac Cx40 channel and thereby cause or confer susceptibility to AF in all of these families.

Only one of the previous described 3 mutations has been studied; L229M. Sun et al., 2013 (A), demonstrated that the mutation L229M is able to form plaque structures localized at the cell-to-cell interface, with some intracellular localization in a very similar manner to WT. They also demonstrated that the L229M mutation doesn't impair the total conductance when the mutation is expressed alone or together with Cx40 WT, but they observed a significant reduction in the conductance when the mutation is co-expressed with Cx43. According with their results this is the first mutation that inhibits Cx43 channel function in a selective way (Sun et al., 2013, A). In the same paper, they also reported a new Cx40 mutation associated with AF, the I75F. This mutation was identified in 1 of 68 patients with alone AF (idiopathic Atrial fibrillation). The mutant channel is able to form GJ plaque-like structures at the cell-to-cell interface in a similar way to WT. Their functional analyses demonstrated that Cx40 I75F is unable to form functional GJ channels though it forms plaques, and that it also impairs coupling when expressed together with Cx40 or Cx43 WT. They also reported that the I75F mutation reduced the total number of active channels without changing the single channel conductance or the gating properties (Sun et al., 2013, A).

In 2012, Makita et al., reported on the mutation Q58L in Cx40 (Fig.8). This mutation was identified in a boy who died at age 11. He had a dominant inherited disorder of the His-Purkinje system, that can lead to severe heart rhythm disturbances. The mutation is also present in his younger sister but she is asymptomatic. The Q58L mutation is predicted to be at the EC1 domain. Functional studies indicated that the expressed protein fails to form GJ plaques even

though the protein is able to reach the membrane. In addition there was a decreased probability for GJ formation in cells co-expressing the Q58L mutant and Cx40 WT (Makita et al., 2012). It is important to mention that this is the first report of a Cx40 mutation associated with a high risk of ventricular arrhythmia (the other Cx40 mutations that have been reported are limited to the atria).

The Cx40 Q49X mutation was identified in 2010 by Yang et al.(Yang et al., 2010 B) (Fig.8). The mutation was found in 7 members of a large Chinese family. The Q49X mutant leads to a premature truncation of the Cx40 polypeptide (Yang et al., 2010 B). Their results indicate that the Q49X mutant is not localized to cell-cell junctions (is not able to form plaques), is unable to form functional GJ channels, and it is retained within the ER (Sun et al., 2014). The Q49X mutant also displays dominant-negative effects on the formation of functional gap junctions when is co-expressed with Cx40 WT or Cx43 WT (Sun et al., 2014).

Guida et al., in 2013 reported the first mutation (P265S) in Cx40 related with tetralogy of Fallot (Fig.8). The mutation was found in two unrelated patients. This mutation is predicted to be at the CT of the Cx in a highly conserved amino-acid position. The mutant channels form only sparse or non-visible plaques and are highly retained intracellularly. Their results show a decrease in LY (Lucifer Yellow dye) transfer in the cell expressing the mutation when compared with cells expressing Cx40 WT. The P265S Cx40 mutation also disrupts the morphology of the heart tube in 37% of zebrafish embryos (Guida et al., 2013).

Atrial Fibrillation

Any deviation from the normal stable heart rhythm is categorized as an arrhythmia (from Greek a + rhythmos= loss of rhythm). Atrial fibrillation (AF) is the most common arrhythmic disorder;

causing morbidity and is a common cause of stroke. AF currently affects ˜3 million Americans, 8.8 million Europeans, and an estimated 30 million individuals worldwide (Tucker et al., 2014). AF is characterized by rapid, seemingly chaotic atrial activation, characterized by the lack of an organized P wave and irregularly irregular ventricular activation (QRSs) (Woods et al., 2014). The causes of AF are multifaceted and may include structural changes in the heart, hypertension and valve diseases. However some AF patients do not have any structural alterations or identifiable underlying diseases, forming a distinct AF subgroup often referred to as idiopathic or lone AF (Delmar and Makita, 2012).

The initiation of an arrhythmia requires a triggering event, and abnormal focal automaticity constitutes a typical trigger. Impulse generation in areas outside the SAN or AVN is called abnormal automaticity, and the site of abnormal pacing is called an ectopic focus. Two triggering mechanisms have been described likely to be the main mechanisms to produce ectopic activity. Early afterdepolarization (EAD's) are inappropriate secondary depolarizations taking place during the normal repolarization phase of the action potential. EAD's are caused when the cell membrane's Ca2+ current recovers from inactivation and allows Ca2+ to move inward (Wakili et al., 2014). EAD's typically originate in ventricular tissue zones, but can also be observed in atrial tissue as triggers of AF. The second proposed mechanism to produce ectopic activity is named delayed afterdepolarization (DAD's). This mechanism is caused by inappropriate activity of the Na+/Ca2+ exchanger (Schmitt et al., 2014).

Persistent or recurrent AF is constantly associated with atrial remodeling. The atrial remodeling is characterized by electrical and structural changes of cardiomyocytes. Electrical remodeling is the consequence of an overall qualitative and quantitative change in ion channel distribution (Schmitt et al., 2014). These changes cause the shortening of the action potential and membrane

hyperpolarization (Muntean et al., 2013). The changes are due to the down regulation of the plateau currents and upregulation of several repolarizing currents. Structural remodeling primarily involves atrial dilatation, hypertrophy, and increased amount and changed distribution of fibrotic tissue not able to conduct electrical signals.

Numerous papers have been published describing different cardiac ion channels mutations related with AF (Table 1). These studies have shown that in most cases AF is associated with mutations in K+ channels that lead to a gain of channel function. This produces a shortening of the atrial action potential duration and the atrial refractory period. It has been demonstrated that the loss of K+ channel function causes a prolongation of the action potential, which results in an early afterdepolarization and AF (Lemoine at al., 2011). Different studies have also demonstrated that mutations in the Na+ channel and in the four sub-units can cause either loss or gain of activity both causing AF. Mutations in different transcription factors related with cardiogenesis like GATA4, GATA5 and GATA6 have been implicated in AF. And in recent years numerous mutations in Cx have been also related with AF.

Hypothesis and Aims

The mutations G38D, A96S and M16V of Cx40 have been implicated in AF. All three mutations retain the ability to form functional channels. The mutant channels, however show different localization patterns within the cell compared with WT. Cx40 WT are localized at the cell-to-cell contact point. Cells expressing the G38D mutant form only sparse plaques. The A96S mutant is localized intracellularly but it does form the same number of plaques as WT. The M163V mutant shows a very similar distribution to that of WT. GJ in the heart control cell-to-cell action potential propagation so the biophysical properties of the GJ are vital to the normal function of the cardiac conduction pathway. We hypothesize that these mutations associated with AF will have different biophysical and expression properties compared to wild type (WT) Cx40.

Specific Aim 1.- Determine the biophysical properties of the channels formed by G38D, A96S and M163V Cx40 mutants. Data from Gollob *et al*.,2006 suggests that the electrophysiological functions of the three mutants are different from the WT. We hypothesize that mutations associated with AF have different conductance and gating properties compared to WT. We will test this hypothesis using the dual whole cell patch clamp technique to investigate the conductance and gating properties between transfected cell pairs.

Specific Aim 2.- Determine the permeability properties of the channels formed by G38D, A96S and M163V Cx40 mutants. It is known that the permeability doesn't depend on the conductance of the Cx. It has been demonstrated that dye transfer is different between various Cx, although the junctional conductance (Vj) of the Cx are similar (Valiunas *et al.*, 2002). The junctional conductance has been shown to be dependent on the size and the charge of the permeant (Imanaga et al., 1987). We hypothesize that mutations associated with AF have different

permeabilities compared with WT. We will test this hypothesis using the dual whole cell patch clamp technique and perforated patch to measure gap junction conductance and at the same time the cellular transfer of Lucifer Yellow (LY) and Ethidium Bromide (EthBr) of the mutants in comparison with WT.

Specific Aim 3.- Determine the protein expression and intracellular traffic of the hemi-channels formed by G38D, A96S and M163V Cx40 mutants. Gollob et al in 2006 showed that the M163V mutant retained the ability to form plaques, the A96S mutant could form small plaques that are small in compared with WT and the G38D mutant didn't show any plaque formation between cells. These mutations in Cx40 could not be only modifying the electrical properties of the channels, but these amino acids changes could also be modifying the protein expression, the protein folding and the intracellular trafficking. We hypothesize that the Cx40 mutations will have different protein level expression and altered traffic to the plasma membrane, possibly causing different electrical and permeability properties.

Figures and Figures Legends

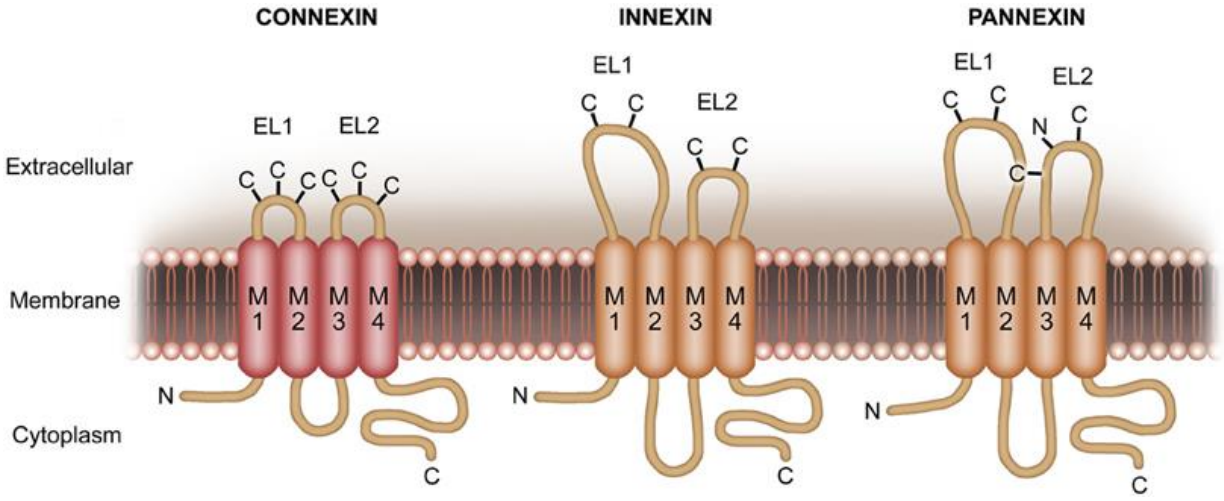

Fig.1.- **Model of Gap Junction Proteins.** All proteins share similar protein topology, 4 transmembrane domains, 2 extracellular loops, one intracellular loop and a carboxy- and amino-termini in the intracellular portion (Prochnow N, 2014).

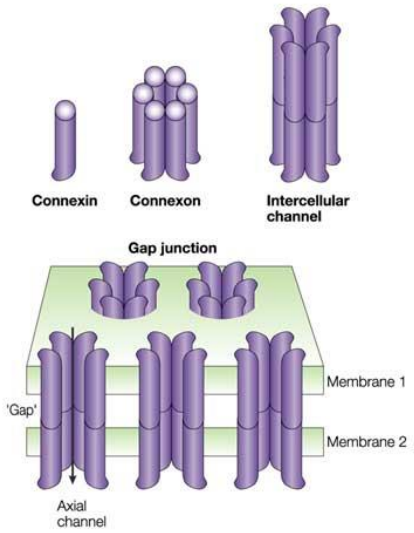

Fig. 2.- **Connexin Gap Junction.** Diagram of the connexin gap junction and the composition of the hemichannel (Goodenough *et al.*, 2003).

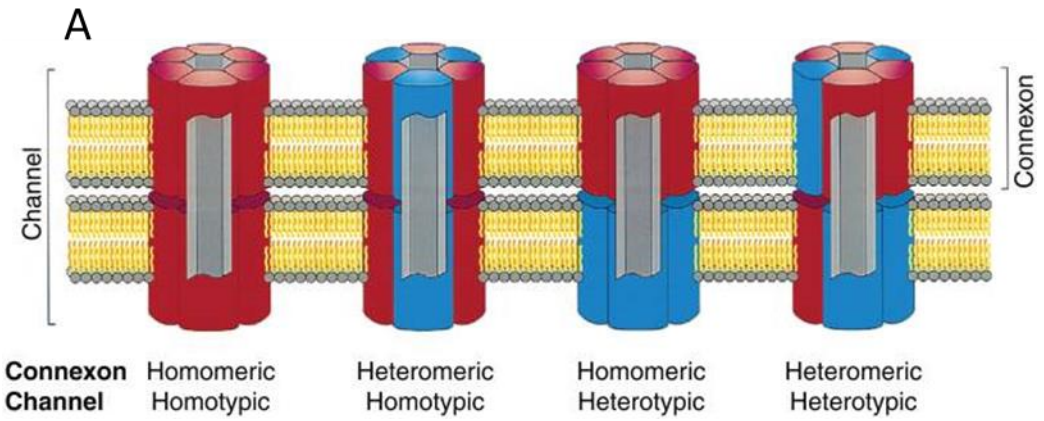

Fig.3.- **Connexon Channels and Connexon Configurations.** A.-Connexons could be homomeric or heteromeric, and gap junction channels could be homotypic or heterotypic (Kumar *et al.*, 1996).

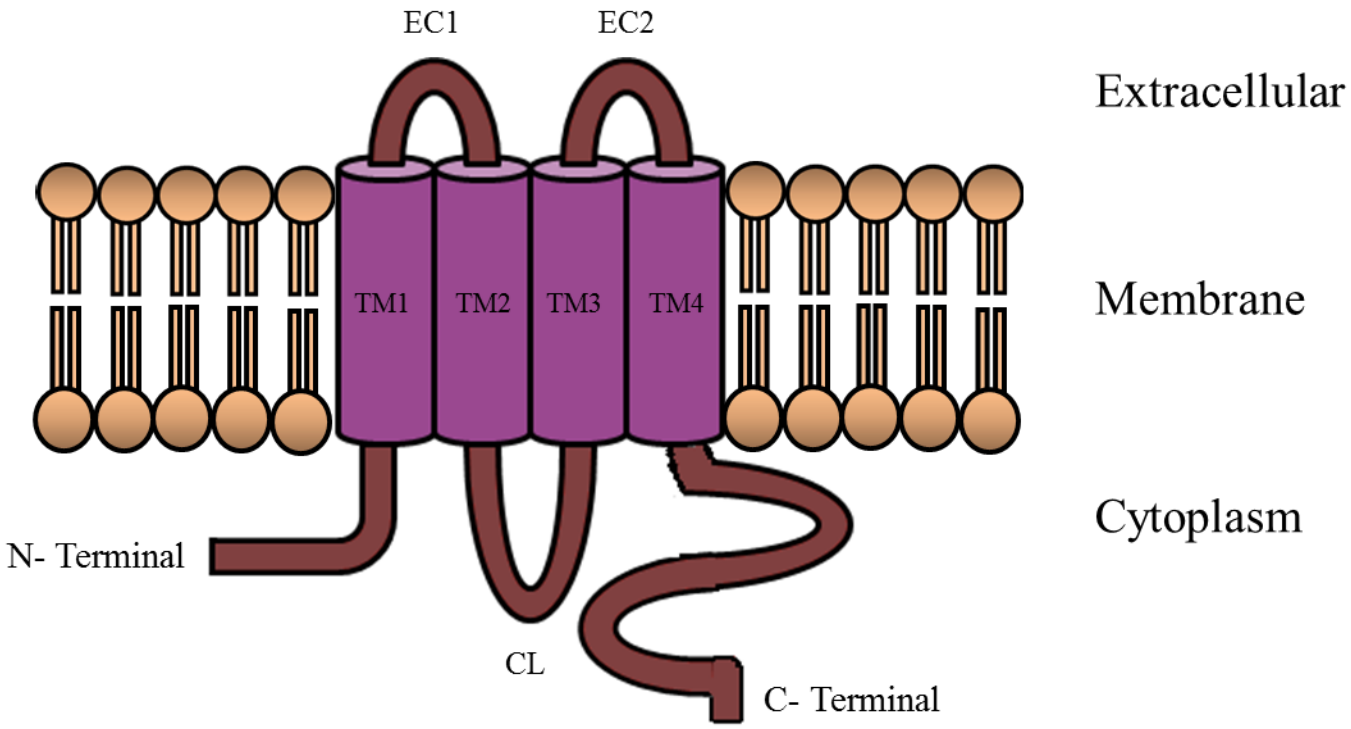

Fig.4.- **Connexin channel topology.** The conexin topology consists of four membrane-spanning segments (TM1-TM4), C-terminal (CT) and N-terminal (NT) domains toward the intracellular side. Three loops connect the transmembrane segments, one cytoplasmic (CL), and two extracellular (E1 and E2).

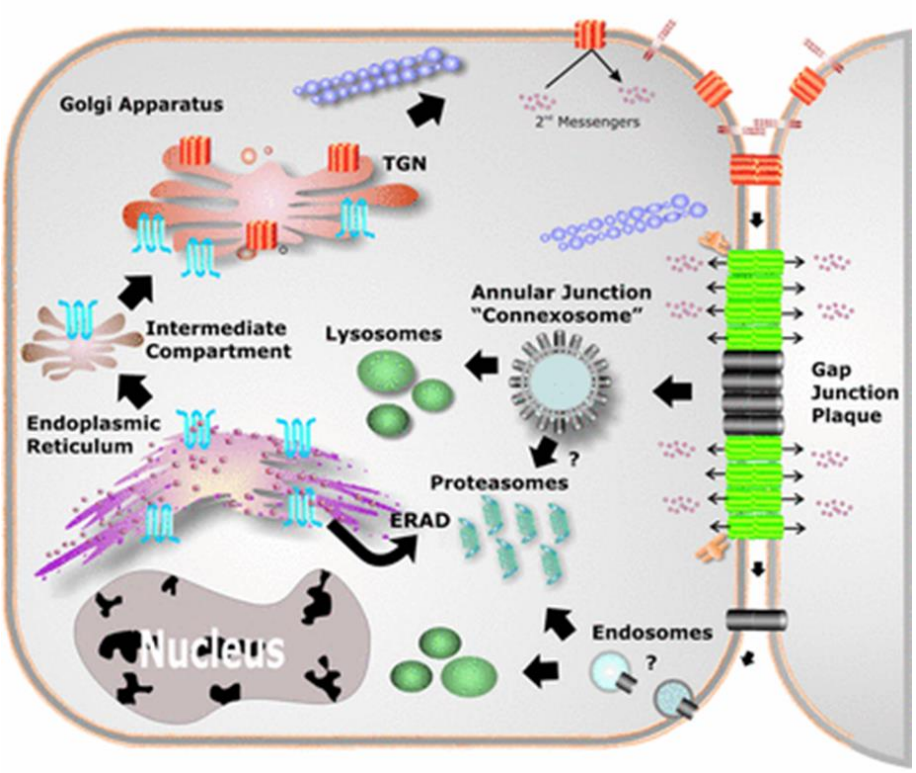

Fig. 5.- **Connexin Formation and Degradation.** Cx are typically co-translationally inserted into the ER. After cross the ER the Cx will pass through the Golgi apparatus in which the Cx will oligomerize. The connexons will be delivery to the cell surface, a process that is facilitated by microtubules. The connexons will diffuse to sites of cell-to-cell contact and dock with connexons from the opposite cell forming a complete channel. The clusters of GJ channels will be name plaques. GJ are removed from the center of the plaque when the plaques are internalized into one of the cells forming an AGJ. AGJ will be targeted for degradation in lysosomes. Adapted from Laird, 2006.

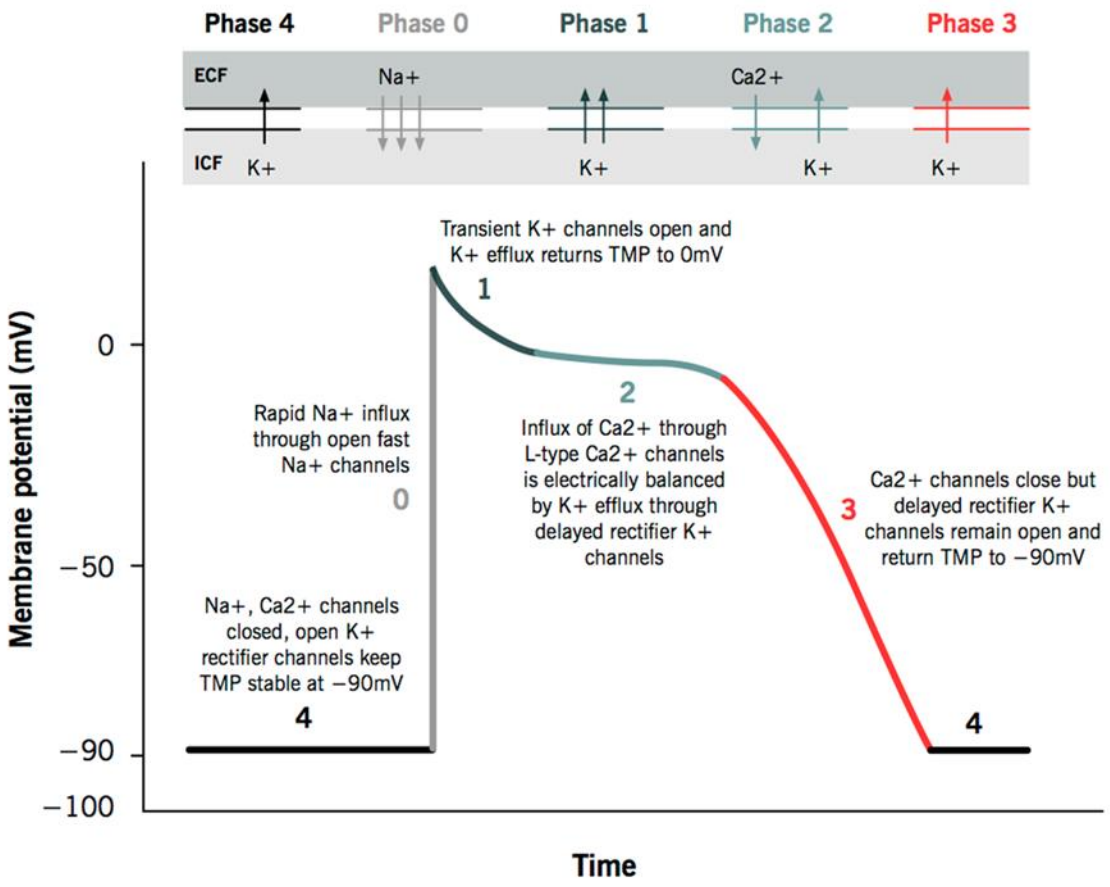

Fig. 6.- **Cardiac action potential.** The action potential in typical cardiomyocytes is composed of 5 phases (0-4), beginning and ending with phase 4. (http://www.pathophys.org/wp-content/uploads/2013/10/ActionPotential.png)

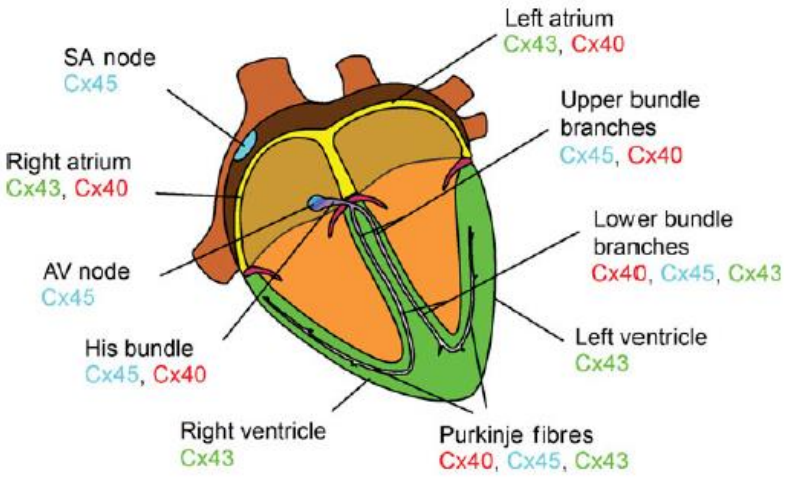

Fig. 7.- **Connexin expression distribution pattern of the mammalian heart** (Severs *et al.*, 2008).

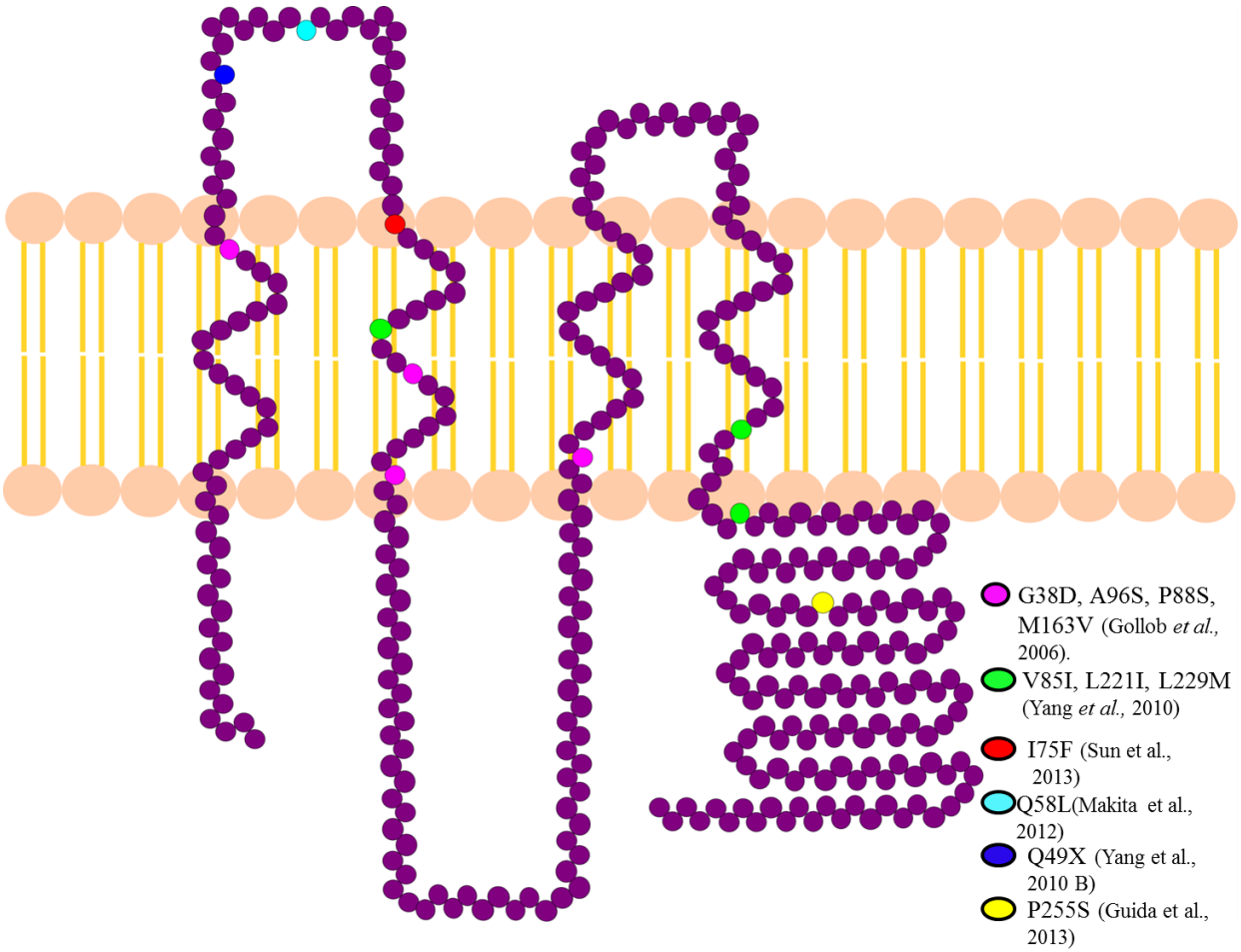

Fig. 8.- **Cx 40 mutations.** Cx40 model with all the Cx40 mutations related with AF. Pink.- G38D, A96S, P88S and M163V mutations described by Gollob *et al.*, 2006. Green.- V85I, L221I, L229M described by Yang *et al.*, 2010. Red.- I75F described by Sun *et al.*, 2013. Cyan.- Q58L described by Maita *et al.*, 2012. Blue.- Q49X described by Yang *et al.*, 2010. Yellow.- P255S described by Guida et al., 2013.

Gene	Gene name	Function
ABCC9	ATP-binding cassette, subfamily C, member9	I_{KATP} current
GATA4	Transcription factor GATA-4	Cardiac development
GATA5	Transcription factor GATA-5	Cardiac development
GATA6	Transcription factor GATA-6	Cardiac development
GJA5	Connexin 40	Formation of atrial gap junctions
GREM2	Gremlin-2	BMP antagonist
HCN4	Hyperpolarization activated cyclic nucleotide-gated potassium channel 4	I_f current
JPH2	Junctophilin-2	Ca^{2+} homeostasis
KCNA5	Potassium voltage-gated channel, shaker-related subfamily, member 5	I_{Kur} current
KCDD3	Potassium voltage-gated channel, shaker-related subfamily, member 3	I_{to1} current
KCNE1	Potassium voltage-gated channel, Isk-related family, member 1	K_v channel activity modulation
KCNE2	Potassium voltage-gated channel, Isk-related family, member 2	Kv channel activity modulation
KCNE3	Potassium voltage-gated channel, Isk-related family, member 3	Kv channel activity modulation
KCNE5	KCNE1-like	Kv channel activity modulation
KCNH2	Potassium voltage-gated channel, subfamily H (eag related), member 2	I_{Kr} current
KCNJ2	Potassium inwardly rectifying channel, subfamily J, member 2	I_{K1} current
KCNJ5	Potassium inwardly rectifying channel, subfamily J, member 5	I_{KACh} current
KCNJ8	Potassium inwardly rectifying channel, subfamily J, member 8	I_{KATP} current
KCNQ1	Potassium voltage-gated channel, KQT-like subfamily, member 1	I_{Ks} current
LMNA	Lamin A/B	Nuclear envelope structure

NKX2.5	Homeobox protein Nkx2.5	Cardiac development
NPPA	Natriuretic peptide precursor A	Systemic sodium homeostasis
NUP155	Nucleoporin 155	Nuclear pore formation
PITX2c	Paired-like homeodomain 2c	Great vein development, left-right asymmetry
RYR2	Ryanodine receptor 2	Ca^{2+} release from sarcoplasmic reticulum
SCN1B	Sodium channel, voltage-gate, type I, β subunit	I_{Na} current modulation
SCN2B	Sodium channel, voltage-gated, type II, β subunit	I_{Na} current modulation
SCN3B	Sodium channel, voltage-gated, type III, β subunit	I_{Na} current modulation
SCN4B	Sodium channel, voltage-gated, type IV, β subunit	I_{Na} current modulation
SCN5B	Sodium channel, voltage-gated, type V, β subunit	I_{Na} current

Table 1.- **Compendium of AF genetic variants identify in families and individuals.** Adapted from Tucker *et al.*, 2014.

Chapter II

Biophysical properties of the channels formed by G38D, A96S and M163V Cx40 mutants

Abstract

GJ are integral membrane proteins and the only known cellular structures that allow a direct cell-to-cell transfer of signaling molecules by forming densely packed arrays or "plaques" of hydrophilic channels that bridge the opposing membranes of neighboring cells.

Cell to cell action potential propagation in the heart is mediated through GJ channels that are located in regions called intercalated discs found at lateral cell-to-cell borders in cardiomyocytes. Cx40 deficiency in the heart has been associated with disturbances of sinoatrial electrophysiology, intra-atrial pulse propagation and a prolongation of the PQ interval and QRS duration. These results point to the critical role that Cx40 plays in electrical conduction in the heart. Any alteration in Cx40 function will clearly impact normal cardiac muscle performance.

In 2006 Gollob at al., described tree mutations in Cx40 that are associate with atrial fibrillation. The mutations are: G38D, A96S and M163V, all mutations form functional channels in vitro.

In this study, the biophysical properties of mutant gap junctions were determined in transiently transfected HeLa and N2A cells using the dual whole-cell patch-clamp technique. The G38D, A96S and M163V Cx40 mutations showed a gj ranges (when expressed in HeLa cells) from 7.5 pS (A96S), 7.4 pS (G38D) and 6.7 pS (M163V)., the gj of these mutants are very similar to the WT 6.6 pS. However, unitary conductance of G38D channels expressed in N2A cells was 1.62

fold higher than the wild-type Cx40 channel (~220 pS versus ~135pS). The A96S and M163V mutants exhibited unitary conductances comparable to the wild-type Cx40 (130-140 pS).

Introduction

GJ channels provide one of the most common forms of intracellular communication and fulfil similar functions in all multicellular animals (Herve and Derangeon, 2012). A single junctional channel is composed of two hemichannels, one in each membrane, that are tighly docked head to head (Gonzalez et al., 2007). Each hemichannel is formed by six connexins. Cxs are multipass transmembrane proteins with both the N- and C-termini oriented towards the cytosol (Koval et al., 2014). The junctional channels could be: homomeric junctional channels when two end-to-end hemichannels spanning two membranes, entirely composed of a single Cx isoform. Heterotypic junctional channels when each hemichannel is composed of a single Cx isoform but different isoforms compose the two hemichannels. Heteromeric hemichannels are hemichannels composed for more than one Cx isoform, so junctional channels could be formed by heteromeric hemichannels (Harris AL, 2001).

The level of communication between cells coupled through GJ is measured electrically by determination of the total conduction of the junction (gj), which is directly related to the product of the total number of channels (N), the unitary conductance (γj) and the open probability of each channel (Po) (Moreno and Lau, 2007). Gj channels exhibit a property common among ion channels whereby conductance is sensitive to voltage (Bakauskas and Verselis, 2004). For this reason, voltage sensitivity is particularly important in regulating the intracellular coupling between excitable cells.

GJ channels provide a direct pathway for electrical and metabolic signaling between adjacents cells (Rackauskas et al., 2010). In cardiac muscle GJs ensure a proper propagation of the electrical impulse which triggers sequential and coordinated contraction of the cardiomyocytes

(Noorman et al., 2009). Cardiac tissue from most mammalian species expresses similar types of connexins: Cx40, Cx43 and Cx45 (Moreno AP, 2004). The expression of these connexins is dynamic in different parts of the heart, and the expression pattern is well conserved among species (Benes et al., 2014). Connexin 40 is the major atrial connexin together with Cx43 (Vozzi et al., 1999). Cx40 is also expressed in the SAN (Kreuzberg et al., 2009), atrioventricular node (Greener et al., 2011), and the His bundle (Greener et al., 2011) and in the Purkinje system (Kreuzberg et al., 2009). Cx 43 is expressed in the atria (Vozzi et al., 1999), in the His bundle (Greener et al., 2011) and in the Purkinje system (Kreuzberg et al., 2009). Cx 45 is expressed in the sinoatrial node (Kreutberg et al., 2009), the atrioventricular node and at the Bundle branches (Greener et al., 2011).

The anisotropic conductive properties of the myocardium are dependent on the geometry of the cardiomiocytes and the number, size and localization of the GJ channels between them. When a depolarizing current is generated, it is divided between charging the membrane nearby and depolarizing the adjacent cell through GJ (Dhein, 2006). In general, cardiac cells express GJ near Na+ channels and at higher densities toward the ends of cells rather than their lateral margins, resulting in lower Ra (axial resistance) and hence faster conduction in the longitudinal direction (Kumar and Gilula, 1996). The resistance of GJ makes up approximately half of the longitudinal resistance in rat atria (Fry *et al.*, 2012), so the conductance of Cxs and therefore GJ help determine the magnitude of Ra and are an important determinant of the conduction velocity. Experiments and simulations demonstrated that conduction velocity is reduces by a decrease in GJ conductance but the change in the GJ conductance should be very large in order to affect the conduction velocity. Experiments with Cx43 have been showed that only when Cx43 was reduced by ≈90%, the conduction velocity slowed by 50% (Gutstein *et al.*, 2001)

The Cx40 gene has been characterized and cloned from several species. Cx40 channels are mildly sensitive to Vj with a half-maximal inactivation at +/- 50 mV (Beblo et al., 1995). Depending on the composition of the pipette solution, single channel recordings in transfected cell lines show a variety of large conductance from 120-200 pS. Sequence analysis of the cytoplasmic loop and the carboxy-terminus has revealed multiple consensus motifs for phosphorylation by several intracellular protein kinases (Kemp and Pearson, 1990). Western blot analysis showed that Cx40 indeed exist in a phosphorylated and non-phosphorylated configuration (Van Rijen et al., 2000).

Given the central importance of Cx in cell-to-cell coupling, changes in Cx expression and distribution would be expected to have profound influences on cardiac conduction (Kato et al., 2012), resulting in different types of cardiac disease like sudden cardiac death and arrhythmias. Different groups have been investigating Cx40 expression and distribution in humans during atrial fibrillation. Some studies show an increase in the protein expression of Cx40 and an heterogeneous distribution during atrial fibrillation (Dupont et al., 2001), while other groups report a decrease in the Cx40 protein with a homogenous distribution during the atrial fibrillation (Wilhelm et al., 2006). The different studies show wide variations, with opposing results even within the same models.

Different Cx40 mutations have been related with atrial fibrillation. AF is characterized by a rapid and irregular electrical activation and the loss of synchronized atrial muscle contractility. Conduction of the action potential in the heart depends on the proper activation of the cardiac Na+ channel and the effective propagation of this by the GJ channels. As mentioned before Cx40 is predominantly expressed in the atria and the His-Purkinje system and is very important in the maintenance of normal action potential propagation in the specialized conduction system of the

human heart. In 2006 Gollob et al. described four mutations in Cx40 that are associated with atrial fibrillation: G38D, P88S, A96S and M163V. The mutations G38D, A96S and M163V form functional channels but the P88S mutation channels are non-functional or the conductance is minimal. These data suggests that the conductance and gating properties of the three mutations that forms functional channels could be different from the WT.

In this study, the biophysical properties of mutant gap junctions were determined in transiently transfected HeLa and N2A cells using the dual whole-cell patch-clamp technique. The G38D, A96S and M163V Cx40 mutations showed a gj ranges (when expressed in HeLa cells) from 7.5 pS (A96S), 7.4 pS (G38D) and 6.7 pS (M163V)., the gj of these mutants are very similar to the WT 6.6 pS. However, unitary conductance of G38D channels expressed in N2A cells was 1.62 fold higher than the wild-type Cx40 channel (~220 pS versus ~135pS). The A96S and M163V mutants exhibited unitary conductances comparable to the wild-type Cx40 (130-140 pS).

Experimental Design

The biophysical properties of Cx40 mutants were determined using dual whole-cell patch-clamp. The measurements will be done in transiently transfected HeLa or N2A cells.

The GJ conductance was measured in HeLa cells pairs transfected with Cx40 WT, G38D, A96S and M163V DNA, using the dual whole-cell patch-clamp technique. Glass cover slips with attached cells were placed in the perfusion chamber of an invert microscope Olympus IX. The external solution (Tyrode solution) contained (mM): 137.7 NaCl, 5.4 KCl, 2.3 NaOH, 1 MgCl2, 10 Glucose, 5 HEPES, and 2mM of BaCl and CsCl were added, the pH was adjusted at 7.4 with NaOH. Patch pipettes were pulled from glass capillaries with an horizontal puller (Sutter Instruments) and filled with internal solution containing 120 mM aspartic potassium salt, 5mM HEPES, 3 mM Na ATP, 10 mM EGTA, with pH adjusted to 7.2 with KOH.

To record the junctional conductance both cells in a pair were clamped at the same potential by two different Axopatch 200B amplifiers (Axon Instruments) controlled by a PC through a Digidata 1440A (Axon Instruments) interface. Voltage steps of 10 mV increments from 110 to -110 mV were applied to one cell, whereas the current produced by the change in the voltage was recorded in the second cell. All experiments were performed at room temperature. The junctional conductance (Gj) was calculated by dividing the measured current (Ij) by the voltage difference,

$$Gj=Ij/(V1-V2).$$

To determine voltage gating properties, currents were measured at the end of the voltage pulse, at the time they approached to the steady state, then the macroscopic conductance was calculated by dividing Ij by Vj, normalized to the values determinate at ±10 mV, and plotted against Vj. This data were fit to a Boltzmann equation of the form:

$$G=(1- Gmin)/((1+exp(-A(Vj-Vo)))*(1+exp(A*(Vj-Vo))))+Gmin.$$

Where Gmin is the minimal conductance (voltage insensitive component). $A=nq/kT$ represents the voltage sensitivity in terms of gating charge as the equivalent number (n) of electron charges (q) moving through the membrane, k is the Boltzmann's constant, T is the temperature and Vo is the half deactivation voltage.

Results

Gollob et al. in 2006 related the G38D, A96S and M163V Cx40 mutations with AF showing that these mutations retained the ability to form functional channels. These are single amino acid mutations in the transmembrane domains of the Cx that could have different conductance and gating properties compared with WT. To investigate the conductance and gating properties of these mutations compared to WT, we expressed the mutants in HeLa and N2A cells and we recorded GJ currents using the dual-whole cell-patch clamp technique.

Dual whole-cell patch-clamp recordings from pairs of transiently transfected HeLa cells expressing the G38D, A96S and M163V Cx40 showed junctional conductance ranges from 7.5 ±8 nS for the A96S mutant (n=39), 7.4 ±4.7 for G38D mutant (n=56), to 6.7 ±5.6 nS for the M163V mutant (n=38). The junctional conductance of these mutants are very similar to the junctional conductance of the WT 6.6 ±6 (n=32)(P value = 0.434, one way ANOVA test)(Table II-1). These data suggest that none of the three mutations are affecting the total conductance of channels.

Vj dependent gating was assessed for each mutant. The three mutations G38D, A96S and M163V mutations have very similar voltage sensitivity between then, 52.53 mV for G38D, 49.67 mV for A96S and 48.47 mV for M163V and in compare with WT, 48 mV (Fig. II-1).These results suggest that the G38D, A96S and M163V mutations in the Cx40 are not affecting the voltage sensitivity of the channels.

Our results for macroscopic properties do not show a significant difference either in total conductance and or in voltage dependence between the three mutants and Cx40, suggesting that

the amino acid substitutions are not affecting the macroscopic properties of the channels. However the unitary conductance of G38D channels expressed in N2A cells is 1.62 fold higher than that of the WT Cx40, being 220 pS for the G38D versus 135 pS for the WT. The A96S and M163V mutants have unitary conductances similar to the WT Cx40, being 130 pS for A96S and 140 pS for M163V (Fig.II-2). Figure II-3 summarizes the single channel conductance of the mutants and WT Cx40. These data suggest that even when the mutations are not affecting the total conductance or voltage dependence of the channels, in the case of the G38D, the substitution is affecting the unitary conductance, showing an increase of 85 pS or 1.63 fold higher when compare with WT (140). The A96S and M163V mutants have similar unitary conductances ((130 pS and 140 pS) to the WT (135 pS) suggesting (P non significative) that these two amino acid substitutions don't affect the unitary conductance of the channels.

Discussion

AF is the most common arrhythmia and it is characterized by a rapid and irregular electrical activation and the loss of synchronized atrial muscle contractility. In the heart, intracellular GJ are crucial for conduction of the electric impulse. Conduction of the action potential in the heart depends on the proper activation of the cardiac sodium channel and the effective propagation of this by the GJ channels. Cx40 expressing myocytes are localized predominantly in the atria and the His-Purkinje system and are very important in the maintenance of normal action potential propagation in the specialized conduction system of the human heart. In 2006 Gollob et al., described 4 mutations that are related with AF, G38D, P88S, A96S and M163V. The mutations G38D, A96S and M163V form functional channels but the P88S mutation channels are non-functional or the conductance is too low to measure (Gollob et al., 2006). In this study we examined the G38D, A96S and M163V Cx40 mutants. Our results showed that all three mutations form functional channels, with conductances comparable to the WT. Gollob et al., in 2006 reported that in the G38D mutant the cell-cell coupling occurred at a significantly lower junctional conductance than the WT. However our results show that the total conductance of the G38D mutant compared to the WT Cx40 is not significantly different. It has been reported in a previous study that in N2A cells the total conductance of the G38D (9.69 nS) is even higher than the WT (4.82 nS) (Patel et al., 2014). It has been reported that the A96S mutant constantly demonstrates no or weak cell-cell coupling, as compared with WT (A96S 1.8 nS vs WT 16.5, N2A cells) (Gollob et al., 2006), and Lubkemeier et al, in 2013 reported a total conductance for the A96S mutation of 1.3 nS and a WT conductance of 34 nS . Our study in HeLa cells shows the total conductance of the A96S mutant is similar to the WT (7.5 nS vs 6.6 nS). Finally, the

M163V mutant total conductance in HeLa cells is also similar to the WT, which agrees with a previous study that the cell-coupling properties were similar to those of WT (Gollob et al., 2006). Both this work and a previous study (Gollob et al., 2006) differs from Patel et al. (2014) that found that the conductance of the M163V and G38D are higher than the WT (M163V 6.81 nS, G38D 9.69 nS vs WT 4.82 nS, expressed in N2A cells) (Patel et al., 2014). These differences could be due to the use of different vectors to the Cx40 mutants expression. We used pIRES vector, Patel *et al* (2014)., used a pSFFV-neo, pTracer-CMV2, pEGFP-N1 or 6B-mCherry vector. Patel *et al* (2014)., used an external solution that was a combination of KCl or NaCl. We are reporting at total conductance for the A96S of 7.5 nS. This conductance differs from the one reported by Gollob *et al* in 2006 and Lubkemeier *et al,* in 2013. These differences could be due the use of different cell line, in the case of Gollob, they used N2A, and we used HeLa cells, and in the case of Lubkemeier, they used a mouse mutation and we used a human Cx. The aminoacid sequence of Cx40 human vs Cx40 mouse is 83 % identical (Alignment done with PRALINE program). The difference in the sequence could be changing the electrical properties of the channels. Our results showing that the total conductance of the mutants is not significantly different from the total conductance of the Cx40 WT is important because it has been shown that a reduction in the Gj conductance is contributing to arrhytmogenesis because a reduction in total conductance causes a reduction in CV. The fact that the mutants have similar conductance to WT could indicate that a possible reduction in the CV that could be causing arrthymias is not from a reduction in the total conductance of the GJ channels.

In this study we also examined the single channel conductance of each mutant. The Cx40 G38D mutant single channel conductance is much more higher than the WT (1.63 fold higher), being 220 pS for the G38D versus 135 pS for the WT. The G38D mutation is located at the

extracellular end of TM1 and replaces a short, neutral and flexible amino-acid with one that is large, rigid, and negatively charged. The replacement of Gly (which is used in flexible regions of proteins) for Asp (often observed interacting with positively-charged non-protein atoms) could cause missfolding of proteins, loss of flexibility and extra electrostatic interactions. It is well known that the absence of a β-carbon allows a Gly to adopt a much wider range of backbone conformation angles than is the case for the other aminoacids (Gray and Matthews, 1987). Gly is also by far the most flexible amino acid (Hollingsworth and Karplus, 2011). This Gly may be a functionally relevant hinge, considering that previous studies have shown that TM1 is the most rigid domain of the connexon (Zonta et al., 2012) and EC 1 must interface with the other cell which may require flexibility. So this G38D mutation in a TM segment could affect the shape, charge and hydrophobicity of the pore, altering the unitary conductance of the channel conductance (G38D single channel conductance = 220pS vs WT = 135 pS). An example of similar destabilizations are the G551D and G1349D mutations in the CFTR chloride channel, which cause a misregulation of the channel (Walsh and Smith, 1993). Other examples are the G342A and G344A mutations in the P2X2 channels in which the receptor ability to switch between conformations change (Li et al., 2004).

The A96S mutation is found on the pore-facing side of the TM2 segment, near the intracellular loop. Alanine is a neutral, hydrophobic, non-reactive, amino-acid that can play a role in substrate recognition or specificity, and has been clearly shown to be a helix-forming residue (Rohl et al., 1999). Replacement of alanine to the slightly longer, polar hydrogen bonding Ser may cause different interactions with solutes or other parts of the connexon through hydrogen bonding. The slightly longer conformation of Ser is charged and polar residues are generally considered helix-

destabilizing (Rohl et al., 1999) due to that polar groups close to the peptide backbone interfere with helix formation (Padmanabhan et al., 1996).

The M163V mutant substitutes a hydrophobic amino-acid that is restricted in available side-chain rotamers for an amino-acid that is also hydrophobic, but has a bulky branched side chain that is usually found in hydrophobic cores. This final mutant could remove important long-distance interactions, and hamper local side-chain packing.

The stability of helices depends on both amino acid composition and sequence details. The intrinsic contribution of amino acid residues to helix stability is given by the propagation parameter, w (Alias et al., 2010). According to the propagation parameters Ala provides the most stability to the helix (1.70) and Pro destabilizes the more (< 0.001) (Rohl et al., 1996). The mutation G38D increases helix stability from 0.048 to 0.38, the A96S mutation decreases stability from 1.70 to 0.40 and M163V also decreases stability from 0.65 to 0.25. Any of these three mutations in TM segments could affect the stability of the channels, the shape, charge and hydrophobicity of the pore.

Figures and tables

HeLa cells

Connexin	Cx40 WT	G38D	A96S	M163V
Junctional Conductance (nS)	6.6	7.4	7.5	6.7
Std.dev.	6	4.7	8	5.6
n	32	56	39	38

Table II-1.- Junctional conductance of the Cx40 mutants. HeLa cells. There were no statistically significant differences between group means as determined by one-way ANOVA (P = 0.434).

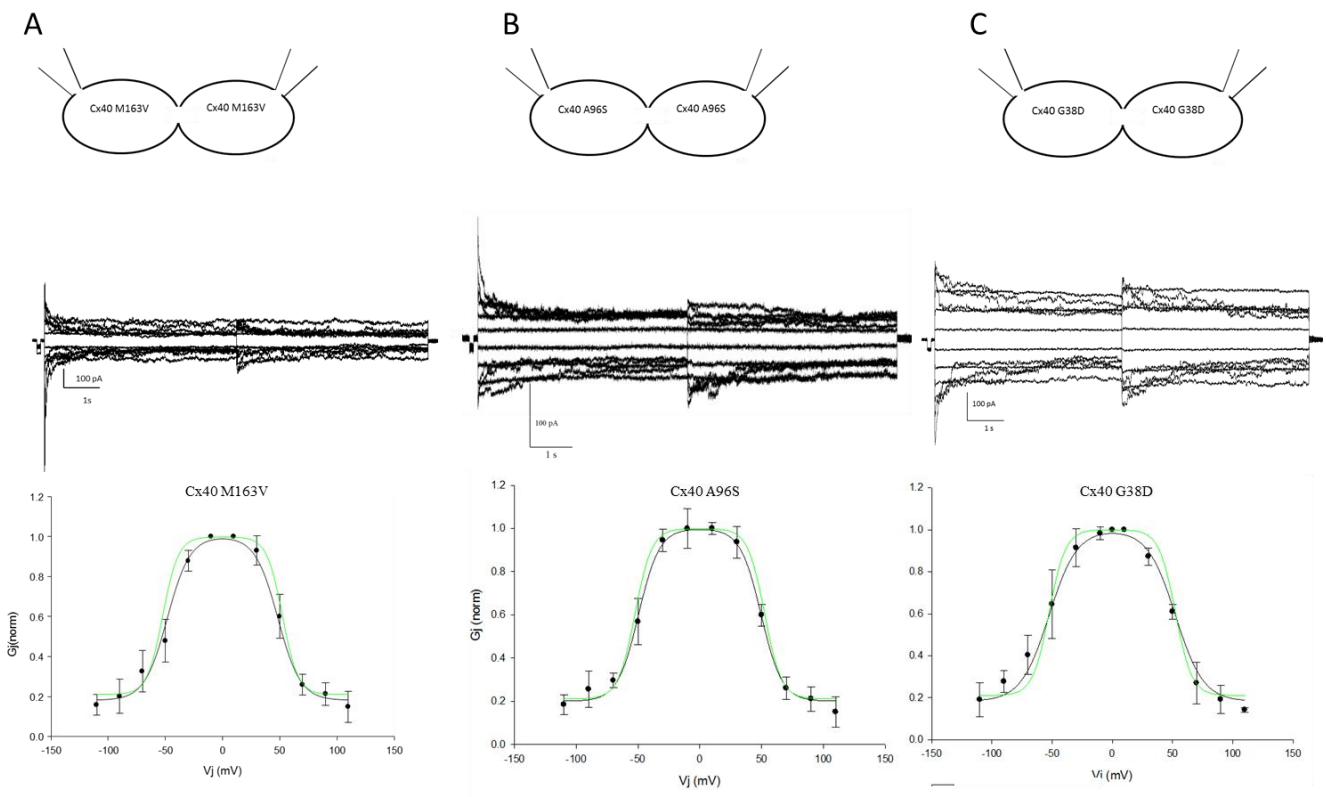

Cx40	Vo (mV)	Gmin	A
WT	48	0.24	0.15
G38D	52.53	0.18	0.08
A96S	49.67	0.20	0.11
M163V	48.47	0.18	0.15

Fig.II-1.- Macroscopic properties of Cx40 mutant gap junctions: M163V (A), A96S (B) and G38D (C). The three columns contain a representation of the cell pairs (top), gap junction currents (middle) and a plot of the normalized conductance (Gj) versus voltage (Vj) (bottom). The lines represent Boltzman fit of the data for Cx40 WT (green line) or for the mutants (black line).Vo, half deactivation voltage. Gmin, voltage insensitive component. A, parameter defining the steepness of voltage sensitivity.

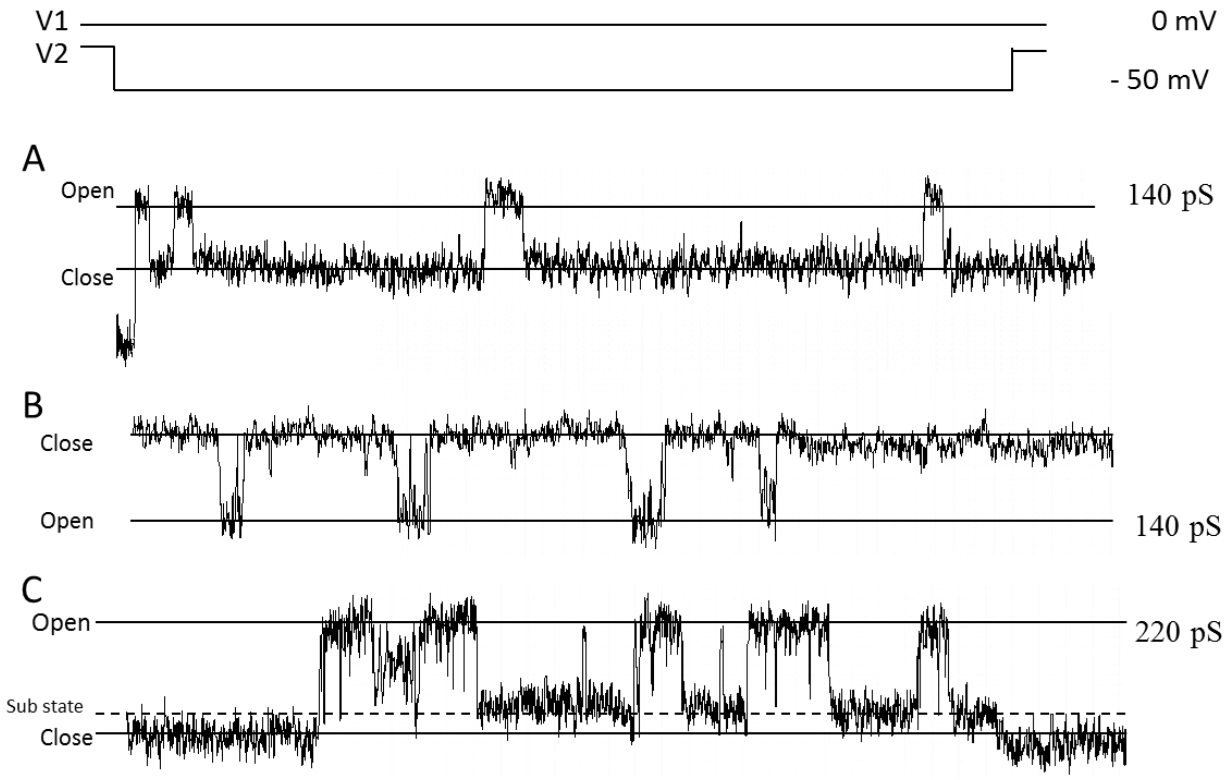

Fig. II-2.- Single channel properties of Cx40 mutants. Representative traces od single channels currents recorded from N2A cells pairs transfected with: M163V, A96S and G38D Cx40 mutants. A.- Cx40 M163V mutant. B.- Cx40 A96S mutant. C.- Cx40 G38D mutant. Solid lines represents the open or close state and dash line represent a sub state.The channels were measure during a 50 mV maintained voltage.

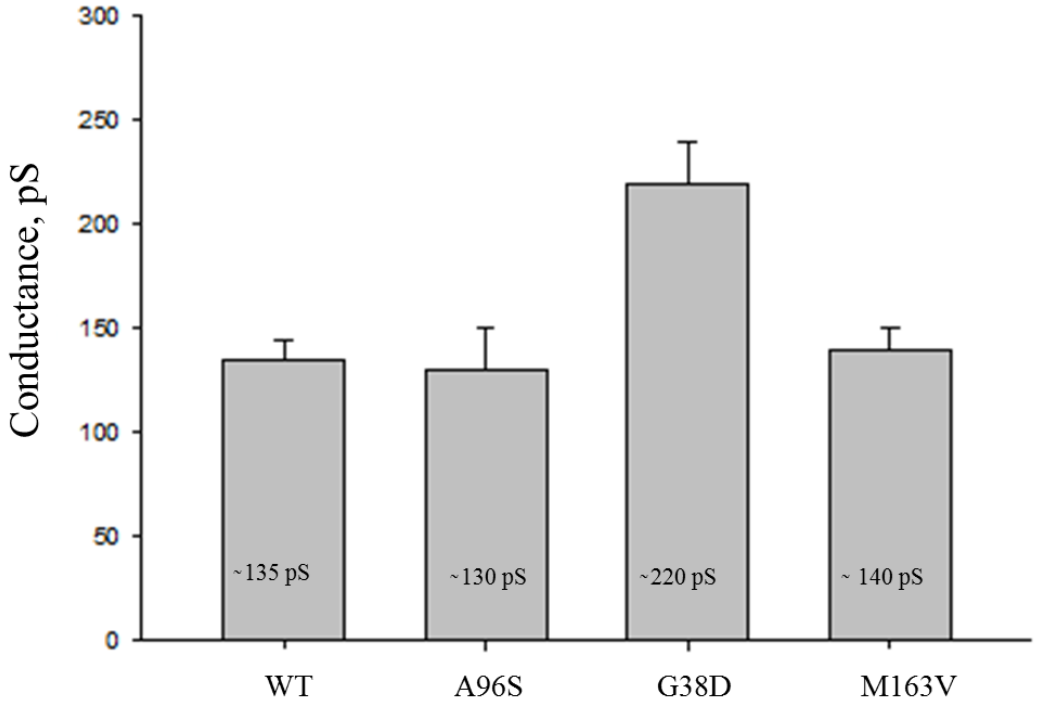

Fig.II-3.- Summary of single channel conductance of Cx40 mutants. Average of single channel conductance of Cx40 M163V (140±10 std., n=30), A96S (130±20 std., n=32) and G38D (220±25std., n=60) mutants.

Chapter III

Permeability properties of the channels formed by G38D, A96S and M163V Cx40 mutants

Abstract

GJ are tightly packed channels that connect the cytoplasm of different cells. These channels not only provide electrical coupling, these channels also provide the pathway that allows the cross of ions, second messengers and metabolites between cells.

Cx40 is mainly express in the Atrium of the mammalian heart, providing a low-resistance pathway for the conduction and propagation of the action potential.

AF is the most common cardiac arrhythmia. A growing number of patients with AF don't present any kind of structural heart malformation or any other cardiac related diseases like hypertension. These suggest that some forms AF could be due mutations in the different cardiac ion channels.

Gollob *et al.,* (2006) identified 4 mutations in Cx40 in patients with alone AF. Only three of the four mutations retain the ability to form functional channels, these mutations are the G38D, A96S and M163V, the last mutation is not able to form functional channels and is the P88S.

In this study, the permeability properties of the Cx40 mutations were tested using dual whole-cell patch-clamp method and perforated patch to measure the GJ conductivity at the same time as the cellular transfer of two different dyes, LY and EthBr. The M163V and the G38D mutation channels exhibited a higher LY permeability when compared with Cx40 WT, while the A96S

mutations showed a similar permeability to WT. In the case of EthBr permeability the M163V and A96S mutations exhibited a higher permeability when compared with Cx40 WT but in this case the G38D mutant is almost impermeable to the dye.

Introduction

The Cx family is composed of transmembrane proteins known to allow direct intracellular exchange of ions and small metabolites by forming Gj channels between neighboring cells (Goodenough and Paul, 2009). The general structure of a Cx consist of four transmembrane domains (TM1-4), two extracellular loops (EL1-2) and one intracellular loop (IL). Both the amino-terminal (NT) and carboxy-terminal (CT) parts of the protein are located in the cytoplasm (Beyer *et al.,* 2012).

While all Gj channels are permeable to current-carrying ions, most of them showing channels conductance values roughly within an order of magnitude irrespective of their Cx composition, their permeability to other substances depends on their Cx composition and varies more widely (Ek-Vitorin and Burt, 2013).

One of the permeability determinats is the gating of the channel. GJ channels regardless of type (homotypic, heterotypic or heteromeric), display voltage-dependent gating, but the kinetics and sensitivity vary over a wide range (Goldberg *et al.,* 2004). GJ channels displays at least one closed configuration and typically more than one open configuration (Veenstra *et al.,* 1995). Haven been also suggest that, under a wide range of intracellular conditions, most GJ channels are gated open more often than closed (Goldberg *et al.,* 2004). In 1995 Veenstra *et al.,* conclude that the selectivity of any given connexin might not correlated with the measured channel

conductance, their results indicate that there is no direct relation between Cx channel conductance and ionic selectivity or dye permeability.

The molecular permeability of the Cx channels have been assessed using several classes of non-biological tracer molecules, usually fluorescent, of widely divergent sizes, charges and chemestries. The permeability to tracers has been assessed in various ways, for example, in the less quantitative assesses counting the number of cells to which dye spreads from a donor cell loaded with a tracer. Another technique that has been use is the Gap-FRAP (FRAP.- fluorescence recovery after photobleach) in which the size and the chemical and biophysical properties of the fluorescent molecules define the communication capacity, allowing quantification of this functionality even if the tracers have no metabolic role. A fluorescent diffusion tracer is first introduced at uniform concentration into all the cells in a tissue culture dish, and a concentration gradient is created by photobleaching the fluorescence in one cell. If the bleached cell communicates with neighbor cells by means of functional GJ channels, resolution of this concentration gradient is detected by monitoring the fluorescence signal, using low-intensity excitation (Abbaci *et al.,* 2008). The technique who gives more data about specific permeability or single channel permeability is using the double patch-clamp method combined with fluorescence microscopy, so combined of those two techniques allow the measure of the Gj conductance while at the same time monitoring the transfer of tracers from one cell to another cell.

Cardiac Gj channels play a critical role in the propagation of action potential by allowing intracellular passage of current-carrying ions. They also are essential for the exchange of larger molecules in both excitable and non-excitable tissues (Valiunas *et al.,* 2002).

The three main Cx isoforms expressed in the heart are Cx40, Cx43 and Cx45. Cx40 is mainly expressed in the atrial myocytes, in the AV-node, His-bundle and the ventricular conduction system. Cx43 is the most abundant and it is expressed in the atrial and ventricular myocytes and distal parts of the conduction system. Cx45 is mainly localized in the SAN, the AVN, His-bundle and bundle branches.

It has been demonstrated that each of the cardiac Cxs (Cx40, Cx43 and Cx45) have different total and unitarian conductance and voltage gating, and also different permeabilities properties. In 2011 Kanaporis et al. reported that Cx40 has very low lucifer yellow (LY) transfer compared with Cx43, Cx45 and Cx26; but Cx40 has similar ethidium bromide (EthBr) transfer with Cx43, Cx45 and Cx26. Their results show that rat Cx40 presents more permeability for negatively charged molecules than for positively charged species, even when both dyes could cross. Rackauskas et al., also reported that the permability of Cx40 to LY is very low compared with Cx43.

In this study, the permeability properties of the Cx40 mutations were tested using dual whole-cell patch-clamp method and perforated patch to measure the GJ conductivity at the same time as the cellular transfer of two different dyes, LY and EthBr. The M163V and the G38D mutation channels exhibited a higher LY permeability when compared with Cx40 WT, while the A96S mutations showed a similar permeability to WT. In the case of EthBr permeability the M163V and A96S mutations exhibited a higher permeability when compared with Cx40 WT but in this case the G38D mutant is almost impermeable to the dye.

Experimental Design

The permeability properties of Cx40 mutants were determined by using dual whole-cell patch-clamp method and perforated patch to measure gap junction conductivity at the same time as the cellular transfer of LY (-2) and EthBr (+1).

Electrophysiological measurements.-The GJ conductance was measure in HeLa cells pairs transfected with Cx40 WT, G38D, A96S and M163V DNA, using the dual whole-cell patch-clamp technique. Glass cover slips with attached cells were placed in the perfusion chamber of an invert microscope Olympus IX. The external solution (Tyrode solution) contained (mM): 137.7 NaCl, 5.4 KCl, 2.3 NaOH, 1 MgCl2, 10 Glucose, 5 HEPES, and 2mM of BaCl and CsCl were added, the pH was adjusted at 7.4 with NaOH. Patch pipettes were pulled from glass capillaries with an horizontal puller (Sutter Instruments) and filled with internal solution containing 120 mM aspartic potassium salt, 5mM HEPES, 3 mM Na ATP, 10 mM EGTA, with pH adjusted to 7.2 with KOH.

To record the junctional conductance both cells in a pair were clamped at the same potential by two different Axopatch 200B amplifiers (Axon Instruments) controlled by a PC through a Digidata 1440A (Axon Instruments) interface. Voltage steps of 10 mV were applied to one cell, whereas the current produced by the change in the voltage was recorded in the second cell. For perforated patch experiments, 30 μM of β-escin was added to the pipette solution. All experiments were performed at room temperature.

Dye flux experiments.- The dye transfer through the GJ channels was investigated using two different dyes, LY (Molecular Probes) and Ethidium Bromide (Molecular Probes). The dyes

were dissolved in internal solution at concentration of 1mg/ml. The transfer was investigated patching one cell with the electrode filled with the mix of internal solution-dye and monitoring the change of fluorescence in both cells over 12 min., after 12 min., the second cell was patch in perforated patch conditions for measure the junctional conductance. The fluorescence in the cells was monitored using a HRm-Axiocam, 14 bit digital CCD-camera. (Fig. III-Exp)

The permeability of a dye molecule is the volume of dye that passes from one cell to the next, over a given unit of time. It has been shown that for the concentrations that we have used, the fluorescence is linearly proportional to concentration (Valiunas *et al.,* 2002). Therefore, the intensity of the dye fluorescence (FI) in each cell is a good proxy for the concentration of the dye in that cell. We have assumed that the concentration of the dye in cell 1, and that the fluorescence (FI_1), has reached steady state and is equal to that of the pipette (Kanaporis *et al.,* 2011).

The gradient for the dye to cross from the donor cell (cell 1) to the recipient cell (cell 2) at one instant is the difference in concentration, represented by fluorescence, between the two cells ($FI_1 - FI_2$). The averaged gradient between time point t and a later time point t+Δt is given by Equation 1 below:

$$\frac{\left(\mathrm{FI}_{1,t} - \mathrm{FI}_{2,t}\right) + \left(\mathrm{FI}_{1,t+\Delta t} - \mathrm{FI}_{2,t+\Delta t}\right)}{2}$$

The averaged gradient of dye between two cells, given above, multiplied by the time between the two measurements (Δt) represents the fluorescence intensity in cell 1 over time Δt (ΔFI_1). The fluorescence intensity in cell 2 over time Δt (ΔFI_2) can be calculated by Equation 2 below:

$$\Delta \mathrm{FI}_2 = \mathrm{FI}_{2,t+\Delta t} - \mathrm{FI}_{2,t}$$

The permeability of the entire GJ can be calculated by multiplying the relative fluorescence intensity ($\Delta FI_2 / \Delta FI_1$) by the volume of cell 2 (V_2). The volume of cell 2 was assumed to be ~1.8 pL, consistent with previous research (Kanaporis *et al.*, 2011). The single channel permeability ($P\gamma$) can be found by dividing the total GJ permeability by the number of active channels, N. The single channel permeability of each dye is found by solving Equation 3 below:

$$P_\gamma = \frac{V_2 * (FI_{2,t+\Delta t} - FI_{2,t})}{\Delta t * \left(\frac{(FI_{1,t} - FI_{2,t}) + (FI_{1,t+\Delta t} - FI_{2,t+\Delta t})}{2}\right) * N}$$

The number of dye molecules that diffuse through a single GJ each second ($N\gamma$) can be calculated in a similar manner. Because the fluorescence of the dye is linearly proportional to the concentration, at a given time point (Δt) the ratio between the fluorescence intensity of the two cells is proportional to the ratio between the concentrations of dye between the two cells. This is represented by:

$$\frac{FI_{2,\Delta t}}{FI_{1,\Delta t}} \approx \frac{C_{2,\Delta t}}{C_{1,\Delta t}}$$

If cell 1 is at steady state, has a dye concentration equivalent to the pipette ($C_{pipette}$), then using Avogadro's constant (N_A), the $N\gamma$ for a given dye can be found by solving Equation 5 below:

$$N_\gamma = \frac{FI_{2,\Delta t} * C_{pipette} * V_2 * N_A}{FI_{1,\Delta t} * \Delta t * N}$$

It is common to report single channel permeability for dyes divided by the single channel permeability for K^+ (Valiunas *et al.*, 2002). This normalization compensates for the range of single channel conductances found in GJs composed of different Cx proteins. For the 120 mmol of K^+ used, a 23.4 mV step (V_{step}) was taken to be equivalent to a 10x concentration gradient

with the assumption that K^+ is the major current carrier. (Kanaporis *et al.*, 2011)For a monovalent charge carrier, with a known cell-to-cell conductance (ʊ), using the elementary charge (q = 1.6 $*10^{-19}$ C), the single channel permeability for K^+ (PγK) can be calculated using Equation 6 below:

$$P_\gamma K = \frac{V_{step} * ʊ}{q * N}$$

The single channel permeability ratio between a given dye and K^+ must compensate for the different concentrations of dye and K^+. For the conditions described above, the final permeability ratio of dye to K^+ (Dye/K) is calculated using Equation 7 below:

$$Dye/K = \frac{N_\gamma * 0.120}{P_\gamma K * C_{pipette}}$$

Results

It has been demonstrated that the dye transfer is different between various Cx, although the junctional conductance of the connexins are similar (Valiunas *et al.,* 2002). The junctional conductance has been shown to be dependent on both the size and the charge of the permeant (Imanaga *et al.*, 1987). Valiunas *et al.,* (2002) reported that rat Cx40 demostrates very low LY transfer compared with Cx43, Cx45 and Cx26; but rat Cx40 has similar EthBr transfer with Cx43, Cx45 and Cx26 (Kanaporis *et al.*, 2011). These results show that rat Cx40 presents more permeability for negatively charged molecules than for positively charged species, even when both could cross the channel. To investigate the permeability of the G38D, A96S and M163V mutations compared with WT, we expressed each mutant in HeLa cells and we used the dual whole-cell patch-clamp method and perforated patch to measure the GJ conductance and at the same time the cellular transfer of LY and EthBr (Method used in Valiunas *et al.*, 2002).

Our results show that the three mutants are able to transfer the anionic dye LY (Fig.III-1).When we plotted the relative fluorescence intensity of the cells at minute 12 versus the junctional conductance, the Cx40 M163V and G38D mutants LY transfer is higher when compared to WT, while A96S transfer is similar to WT (Fig. III-2). The results from LY transfer experiments suggest that M163V and G38D presents less perm-selectivity for negative charges than WT, when the A96S presents similar perm-selectivity when compared with WT.

The three mutations show different transfer levels of EthBr when compared to WT (Fig. III-3). After plotted the relative fluorescence intensity at 12 minutes versus the junctional conductance, the M163V and A96S mutants show more relative transfer of the dye than the Cx40 WT, and the G38D mutant is almost impermeable to EthBr (Fig. III-4). These results suggest that the mutants

M163V and A96S have less perm-selectivity for positively charged molecules than WT, and that the G38D mutation is affecting the perm-selectivity of the channel making it less permeable to positive charges.

Our data show that the single channel permeability (Fig. III-5) and the permeability of fluorescent probes relative to K+ (Fig III-6) of the mutations is different than the WT permeability. Cx40 WT single channel permeability for LY is 0.88 $x10^{-15}cm^3/s$, which is similar to the single channel permeability for the A96S mutant (1.08 $x10^{-15}cm^3/s$ vs 0.88 $x10^{-15}cm^3/s$). The M163V mutant has a single channel permeability to LY of 1.63 $x10^{-15}cm^3/s$, which is~2 fold higher than that of WT. Finally, the G38D mutant has a single channel permeability to LY equal to 3.05 $x10^{-15}cm^3/s$, which is~3.5 fold higher than WT. The permeability of LY relative to K+ is: WT= 0.0031, G38D= 0.0544, A96S= 0.004, M163V= 0.0066. With these numbers is clear that the LY permeability relative to K+ of the M163V and G38D mutants is higher than the WT, and the A96S is very similar to the WT. For EthBr the Cx40 WT has a single channel permeability of 8.0 $x10^{-15}cm^3/s$. M163V mutant has a single channel permeability of 35.0 $x10^{-15}cm^3/s$, which is 4.37 fold higher than WT. The A96S single channel permeability is also higher than the WT (22.0$x10^{-15}cm^3/s$ vs 8.0$x10^{-15}$ cm^3/s). The single channel permeability of the G38D mutant is smaller than the WT (3.1$x10^{-15}$ cm^3/s vs 8.0$x10^{-15}$ cm^3/s). The permeability of EthBr relative to K+ is: WT= 0.0198, M163V= 0.0575, A96S= 0.0367 and G38D= 0.0014. The permeability of EthBr relative to K+ for the mutants M163V and A96S is higher than the WT and the one for G38D mutant is smaller than the WT.

Discussion

An important functional role for Cx proteins is their ability to form intercellular channels capable of supporting intercellular exchange of molecules up to ~1,000 Da (Harris AL, 2007). Classically, ions and metabolites <1000 Da, (e.g. ATP, Ca2+, cAMP, and IP3), are known to pass through GJ channels. But larger molecules, such as peptides and small nucleotides (such as ATP, cAMP, ADP and siRNA(Valiunas *et al.,* 2005)), have also been shown to be able to diffuse through GJ (Meens *et al.,* 2013). The molecular permeabilities of Cx channels have been assessed using several classes of nonbiological tracer molecules, usually florescent, of widely different sizes, charges and chemistries (Harris and Locke, 2004). In this study we examined the permeability of the Cx40 mutants for two different dyes, different in charge and size, LY and EthBr.

Our result using LY showed a difference in the permeability between the WT and the G38D and M163V mutants. The relative transfer of LY through Cx40 G38D and M163V mutants is higher, when compared to WT(slopes of G38D= 0.016±.0011 nS^{-1} and M163V= 0.007±.0004 nS^{-1} vs WT slope of 0.0020±.0004 nS^{-1})(T-test shows a significative difference between G38D and WT (P=0.0001) and M163V and WT (P=.005) . The difference in the permeability of LY with the M163V and G38D mutants vs. the WT could be explained by a change in the interaction between the molecular probe and the pore walls. The Cx40 M163V mutation could be changing the characteristics of the pore because Val is a short, branched amino acid compared to the Met. This mutation could cause a change in the pore width, changing the permeability properties of the junction. The change of side chains between Gly (neutral amino acid) to Asp (negatively charged amino acid) would likely alter the interaction of the LY with the pore walls (and having

an interaction with the charge of the probe), these differences could be causing the differences in permeability of LY when compared to WT.

In the case of EthBr our data showed that all three mutations have different level of transfer when compared to WT. The M163V and A96S mutants show more relative transfer of the dye than the Cx40 WT (slopes of M163V= 0.0590±.0190 nS^{-1} and A96S= 0.03223±.0041 nS^{-1} vs WT= 0.0078±.0015 nS^{-1}) (T-test shows a significative difference P=.001), and the G38D mutant is almost impermeable to EthBr (slope of 0.0020±.0015 nS^{-1} vs WT= 0.0078±.0015 nS^{-1}). These differences in permeability could be also explained by a change in the interaction between the molecular probes and the pore walls. In the case of the M163V mutant the permeability is much higher than the WT and in general our results showed that in this mutant the permeability for both dyes increases considerably compared that to WT. The M163V mutation is a change from a large, hydrophobic, non-reactive amino acid (Met) to an also hydrophobic but small amino acid, (Val). This change in the size of the amino acids could alter the pore width, causing an increase in the permeability. It is important to notice that this mutation is causing an increase in the permeability of both dyes, suggesting that this mutation is non-specifically reducing selectivity. In the case of the G38D mutant the change of side-chains between Gly a short, neutral and flexible amino acid to Asp a large, rigid and negatively charged amino acid, would likely alter the interaction of the permeant with the pore walls in both, pore size and charge interactions. It is very important to notice that the G38D mutant creates charge selectivity between the dyes, allowing the LY to cross the junction with a high permeability and causing the Cx to be almost impermeable to EthBr. The A96S mutation could be affecting the width of the pore and/or creating different interactions between the permeants and the addition of extra hydrogen bonding options, causing an increase in the permeability for the dye.

While it is important to evaluate the permeability of nonbiological molecules (dyes), it is also important evaluate the permeability of biological molecules such as IP3, cAMP and microRNAs. All of these are involved in cell signaling and could be playing an important role in the development of AF. For example MicroRNAs have been the focus of different investigations in the last few years and their misregulation may important for the development of atrial fibrillation.

Figures and Tables

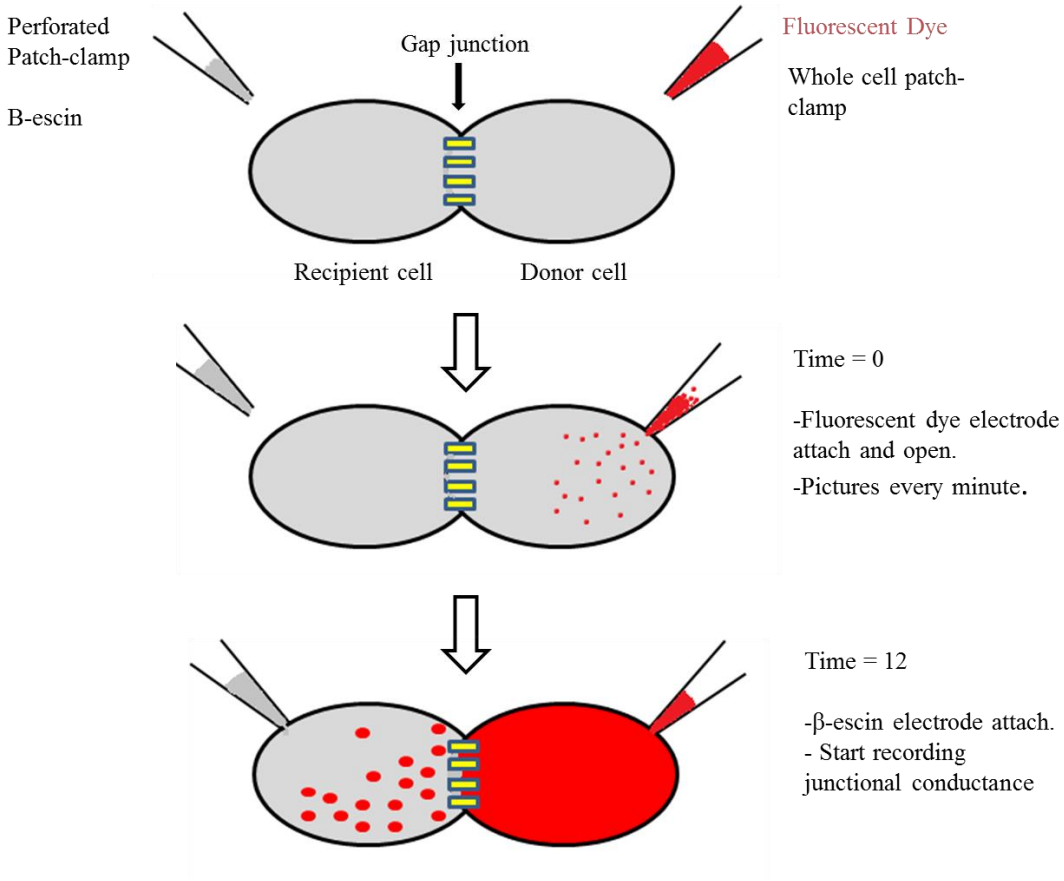

Fig.III-Exp.- Permeability experimental design. Dual whole cell (donor cell) and perforated patch (recipient cell) was use to investigate the dye transfer through the GJ (top). The dye was introduce to the donor cell using a patch pipette, this is min. zero (middle). The change of fluorescence in both cells were monitoring over 12 min., after 12 min., the recipient cell was patch in perforated patch conditions for measure the junctional conductance.

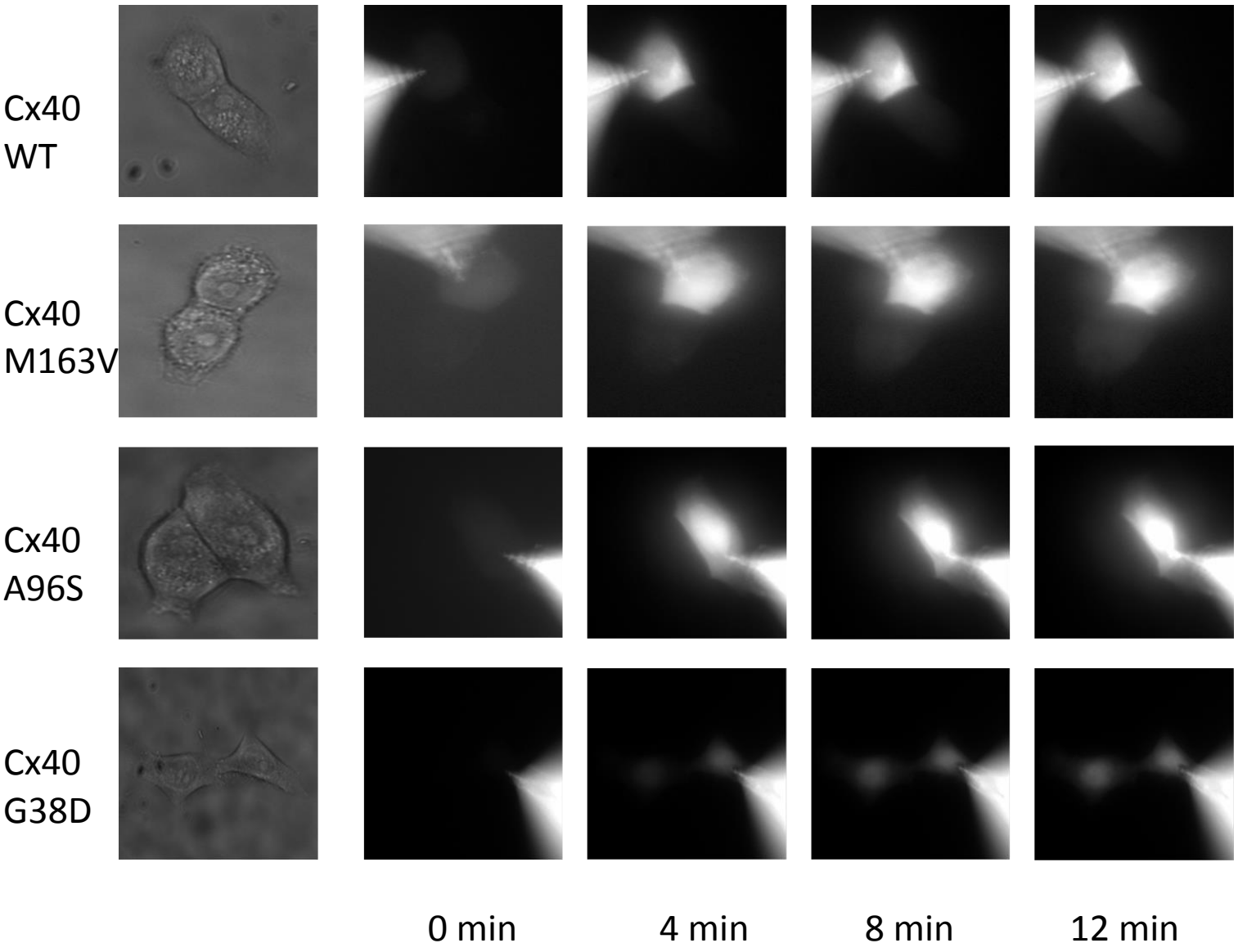

Fig.III-1.- Representative images at different time points of cell to cell transfer of LY. Cell-to-cell transfer of LY in HeLa cell pairs expressing Cx40 mutants M163V, A96S and G38D. The increase of fluorescence intensity in the recipient cell was monitored for 15 min. Representative images at 0, 4, 8 and 12 min are shown. The increase in the intensity reflects the probe transfer from the injected cell to the recipient cell.

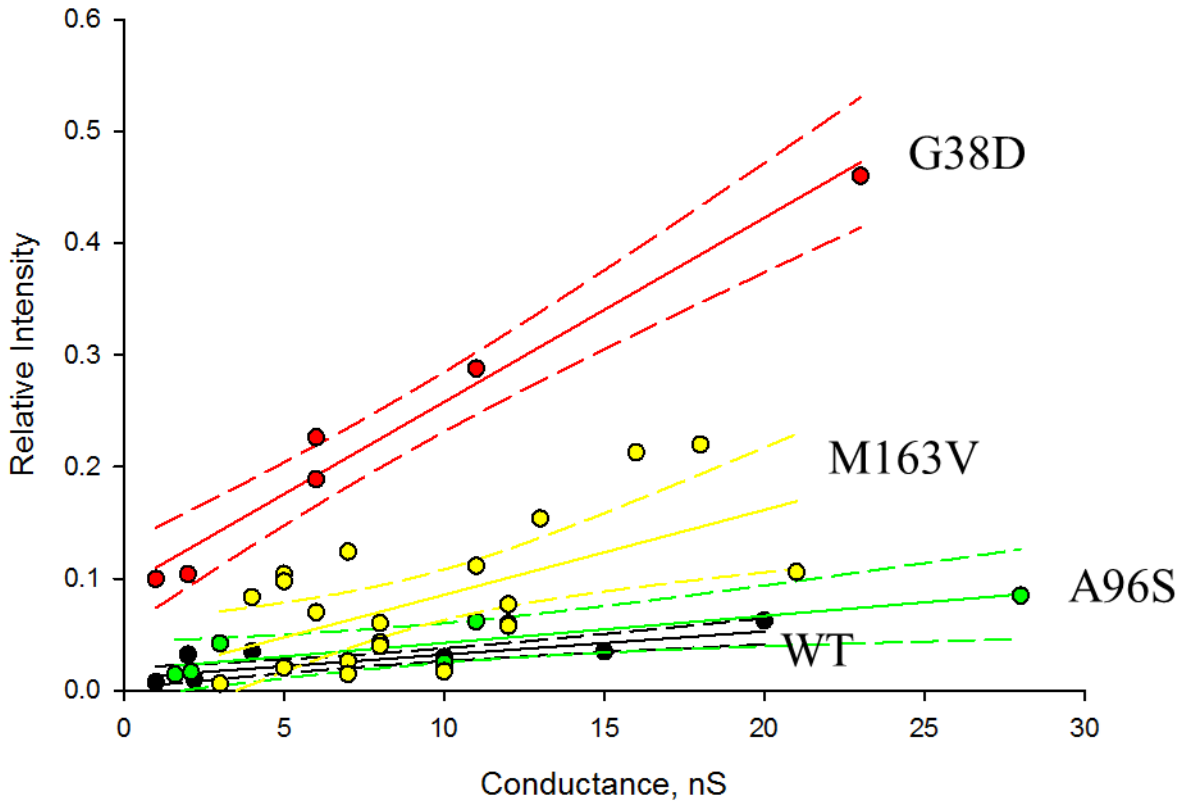

Fig.III-2.- Summary plots of relative intensity versus conductance for LY. Summary plots of relative intensity versus conductance for LY: G38D (red), A96S (green), M163V (yellow) and WT (black). Colored dots are the relative intensity at 12 min. The relative intensity is the fluorescence intensity of the recipient cell over the fluorescence intensity of the dye donor cell. Continuous lines correspond to first-order regressions and dashed lines are 95% confidence interval. First order linear regression slopes: WT (0.0020±.0004 nS^{-1}), G38D (0.0160±.0011 nS^{-1}), A96S (.0024±.0006 nS^{-1}), M163V (0.007±.0004 nS^{-1}).

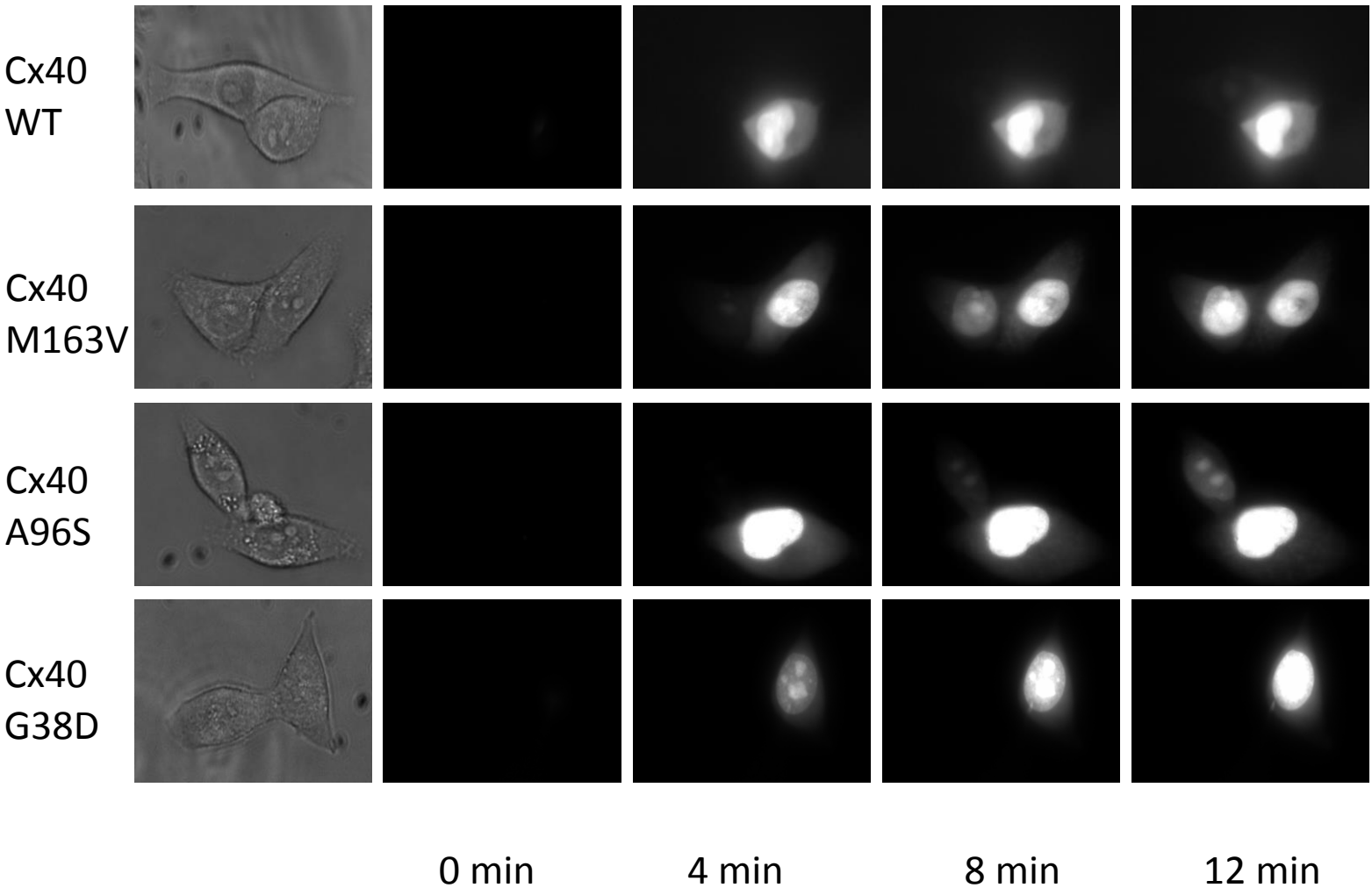

Fig.III-3.- Representative images at different time points of cell to cell transfer of EthBr. Cell-to-cell transfer of EthBr in HeLa cell pairs expressing Cx40 mutants M163V, A96S and G38D. The increase of fluorescence intensity in the recipient cell was monitored for 15 min. Representative images at 0, 4, 8 and 12 min are shown. The increase in the intensity reflects the probe transfer from the injected cell to the recipient cell.

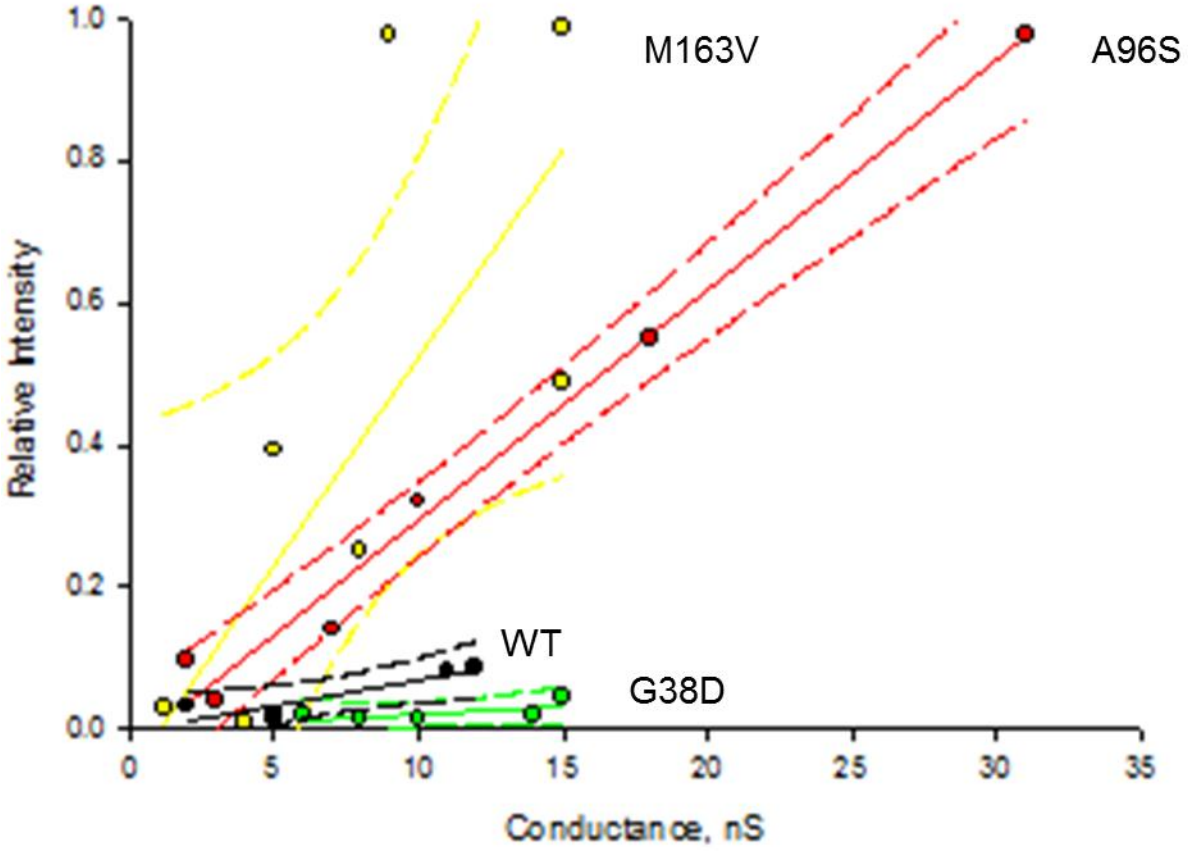

Fig.III-4.- Summary plots of relative intensity versus conductance for EthBr. Summary plots of relative intensity versus conductance for EthBr : G38D (green), A96S (red), M163V (yellow) and WT(black).). Colored dots are the relative intensity at 12 min. The relative intensity is the fluorescence intensity of the recipient cell over the fluorescence intensity of the dye donor cell. Continuous lines correspond to first-order regressions and dashed lines are 95% confidence interval. First order linear regression slopes: WT (0.0078±.0015 nS^{-1}), G38D (0.0020±.0015 nS^{-1}), A96S (.03223±.0041 nS^{-1}), M163V (0.0590±.0190 nS^{-1}).

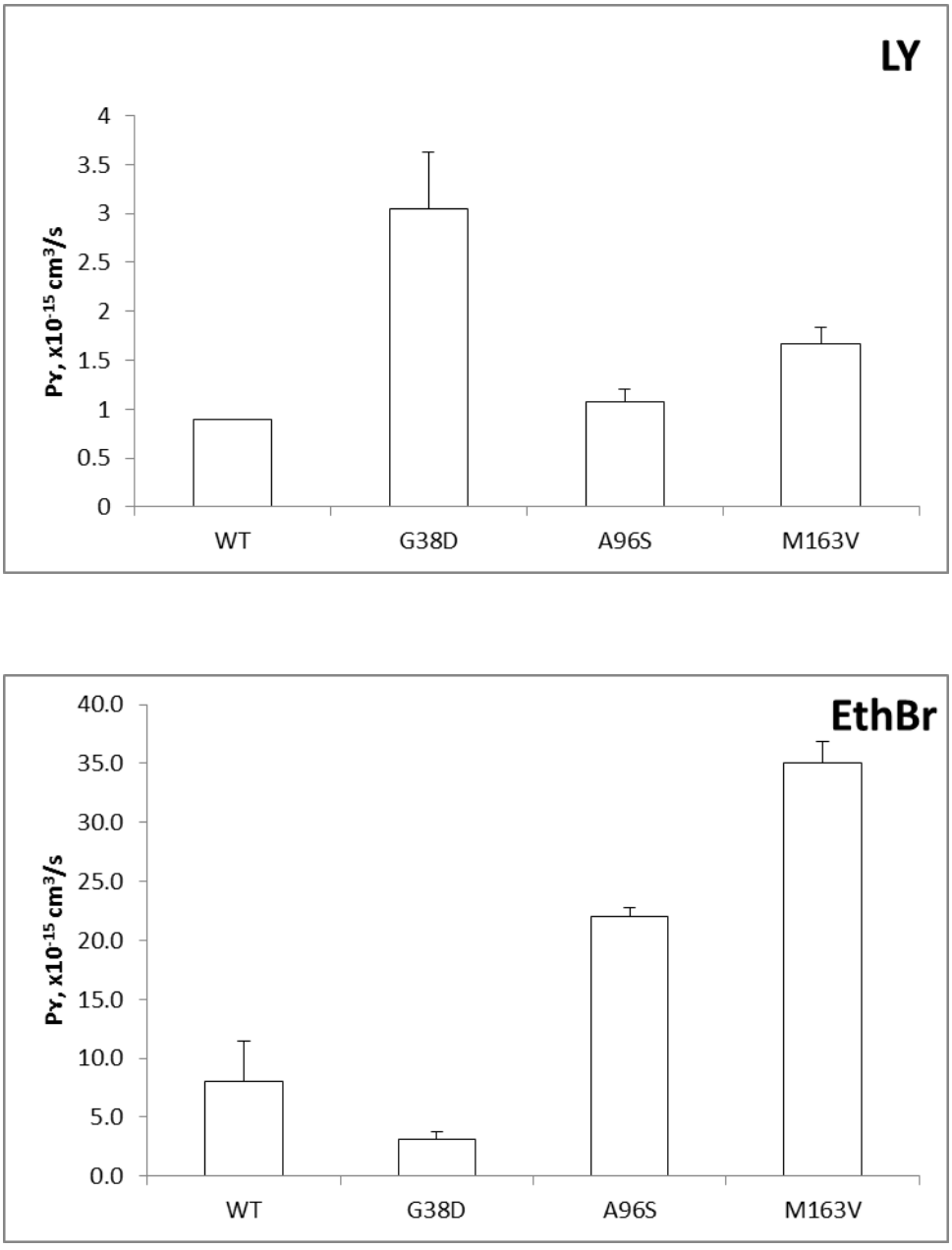

Fig.III-5.- Summary of single channel permeability for Cx40 WT and Cx40 mutants. LY.- WT (.88±.01 $x10^{-15}cm^3/s$), G38D (3.05±1.49 $x10^{-15}cm^3/s$), A96S (1.08±.13 $x10^{-15}cm^3/s$), M163V (1.67±.17 $x10^{-15}cm^3/s$). EthBr.- WT(8.0±3.5 $x10^{-15}cm^3/s$), G38D (3.1±.67 $x10^{-15}cm^3/s$), A96S (22.0±.74 $x10^{-15}cm^3/s$), M163V (35.0±1.95 $x10^{-15}cm^3/s$).

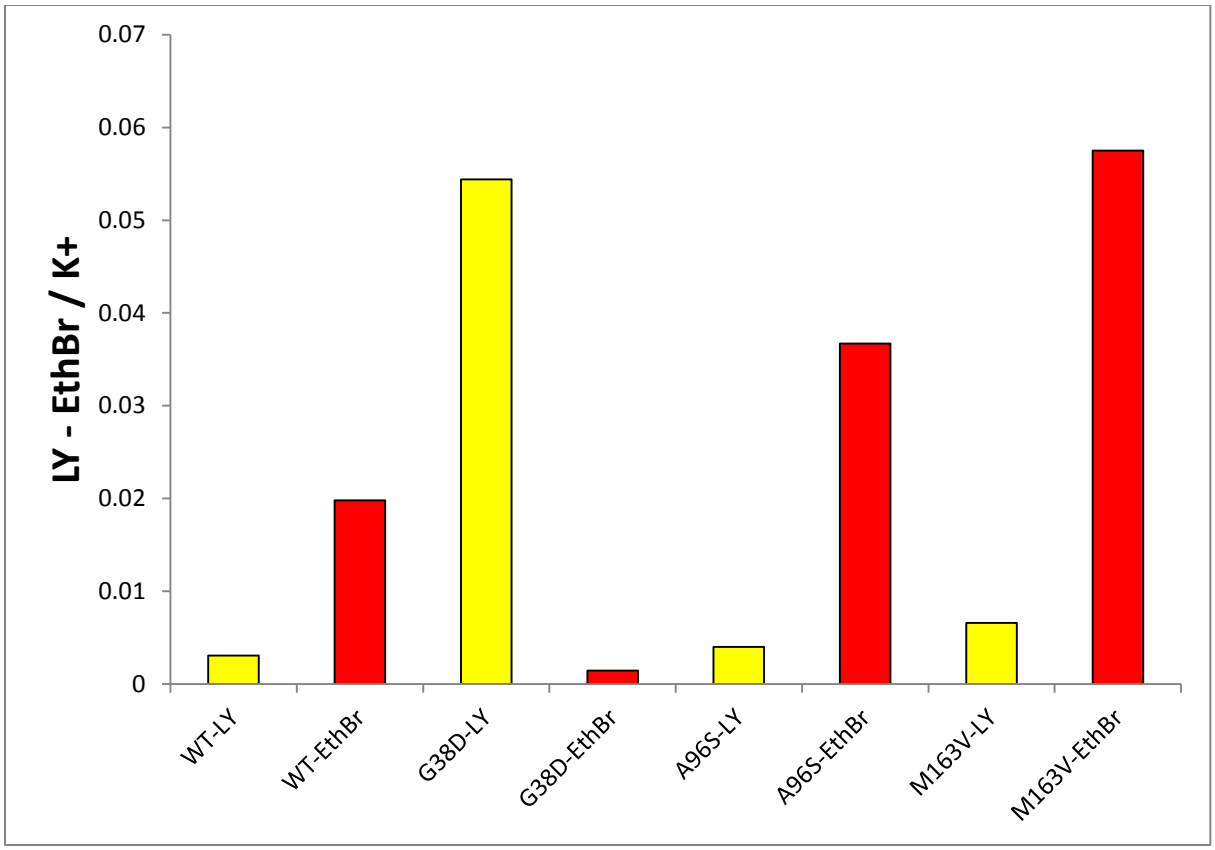

Fig.III-6.- Summary of probe/K+ ratio for Cx40 wild-type and mutants. LY.- WT= .0031, G38D= .0544, A96S= .004, M163V= .0066. EthBr.- WT= .0198, G38D= .0014, A96S= .0367, M163V= .0575.

Chapter IV

Protein expression and intracellular traffic of the hemi-channels formed by G38D, A96S and M163V Cx40 mutants

Abstract

During the last years, several Cx40 mutations have been describe in patients with AF. In 2006 Gollob et al., identified four of these mutations, the G38D, P88S, A96S and M163V Cx40 mutations. Three of these mutations retain the ability to form functional channels, the mutations are: G38D, A96S and M163V. Gollob et al., also reported that the A96S and M163V are able to form plaques between cells but they couldn't find any kind of plaque formation with the G38D mutant. Here we tested the total protein level of the mutants in compare with Cx40 WT, their ability to form plaques between cells, and their co-localization with the Golgi apparatus and with the early endosome. The mutants protein level were test using the Western blot technique. The G38D and A96S mutants showed similar amount of protein in compared with WT but the M163V mutant showed a higher level of protein in compar with WT. The ability of the mutants to form plaques and their co-localization with the Golgi apparatus and early endosome were tested using immunofluorescence labeling. The immunofluorescence microscopy for Cx40 WT showed that the Cx form a well-defined plaque between cells, that the Cx co-localizes with the Golgi apparatus and with the early endosome. The M163V mutant is able to form plaques, it showed some co-localization with the Golgi and with a higher concentration in the early

endosome in compare with the Cx40 WT. The A96S mutant is also able to form plaques between cells, co-localize with the Golgi and the co-localization with the early endosome is very high when compare with the Cx40 WT. The G38D mutant is also able to form plaques, co-localize with the Golgi and was found in a very high concentration at the early endosome in compare with Cx40 WT.

Introduction

GJ are specialized regions of cell-to-cell contact at which hexameric oligomers, called connexons, dock end-to-end noncovalently across a narrow extracellular gap (Yeager and Harris, 2007). Gap junctions allow the direct exchange of ions, such as K+ and Ca2+, second messengers, such as inositol triphosphate, ATP, cAMP and cGMP, and small metabolites, including glucose and glutamate (Leithe et al., 2012).

GJ are comprised of integral multi-pass transmembrane proteins called connexins (Nielsen at al., 2012). The topology of a connexin subunit consist of four membrane spanning segments (TM1-TM4), with N terminal and C terminal domains located intracellularly and two extracellular loops, connecting TM1 to TM2 and TM3 to TM4. Each connexon, or hemichannel, is an annular assembly of six individual connexins that forms a pore through the plasma membrane (Yeager and Harris, 2007). The connexons are homomeric when they contain only one Cx type or heteromeric when they contain different Cx. When the GJ is formed by two identical connexons they are named homotypic channels; and when the channel is formed by two different connexons they are named heterotypic channels.

Cx have a short half-life of only 1-5 hrs (Berthoud et al., 2004).Cx are generally considered to be co-translationally inserted into the ER membrane (via the translocon and encoded start and stop transfer sequences), although cell-free studies indicate that Cx26 can also insert into membranes post-translationally or directly into the plasma membrane (Zhang et al., 1996). After be co-tranlationally inserted into the ER, the Cx are properly folded with the assistance of molecular

chaperones. Cx oligomerization is connexin-type dependent, for example Cx32 assembles in the ER while Cx43 assembles in the trans-Golgi network.

Cx with correct conformation are transported via the Golgi apparatus and the trans-Golgi network to the plasma membrane; some studies have been reported that Cx26 could reach the membrane via Golgi-independent pathway (George et al., 1999). Cx are delivered to the plasma membrane at non-gap junctional sites, and diffuse laterally to the periphery of the GJ plaques where they dock with connexons in neighboring cells to form intercellular channels (Leithe et al., 2012). Older GJ are removed from the center of the plaque by the internalization of double membrane structures called connexosomes or annular gap junctions (AGJs). This internalization occurs through a combined endo/exocytic process, because one of the cells (acceptor cell) will accept part of the membrane of the other cell (donor cell) (Falk et al., 2014).

The degradation of the GJ could follow two pathways; the proteasomal and the endo/lysosomal degradation pathways.

The proteosomal pathway is the route of degradation for cytosolic and nuclear proteins (Berthoud et al., 2004). The proteasome is a 26S holoenzyme complex comprised of 2 major subunits, the 20S core, which contains the proteolytic activity, and the two 19S cap or regulatory particles which are each made up of multiple individual protein subunits (Voges et al., 1999). Proteasomal degradation could be ubiquitin-dependent or independent. Ubiquitination is essential for the proteolysis of proteins, during both constitutive degradation and degradation as a result of changes in the extracellular environment. Ubiquitination occurs through a sequential activation of three classes of enzymes. First, a ubiquitin-activating enzyme, called E1, forms a thiol-ester bond with the C terminus of ubiquitin (glycine76). Then, a ubiquitin-conjugating

enzyme, known as E2, accepts ubiquitin from E1 by a trans-thiolation reaction. Finally, a ubiquitin ligase, known as E3, catalyzes the transfer of ubiquitin from the E2 enzyme to the substrate protein. E3s specify the timing and substrate selection of ubiquitination reactions and are therefore the key regulatory determinants in the ubiquitination process (Kjenseth et al., 2010). ER-associated degradation (ERAD) is the process responsible for the removal and proteasomal degradation of misfolded proteins localized to the ER. During ERAD, misfolded proteins in the ER are recognized by a molecular chaperone such as Bip, transported out of the ER through the retrotranslocon channel into the cytoplasm to be degraded by the proteasome (Su and Lau, 2012).

The lysosomal pathway has two different degradation pathways, the endo-/lysosomal and the phago-/lysosomal (termed macroautophagy). The endo-/lysosomal pathway is design for the uptake of extracellular nutrients and factors via the formation and internalization of vesicles from the plasma membrane (Falk et al., 2014). It has been proposed that after the AGJ formation, the inner AGJ membrane splits and peels away from the outer AGJ membrane, generating a single-membran cytoplasmic AGJ vesicle that then can fuse with a single-membrane endosome (Kjenseth et al., 2010). This single membrane can now be degraded via the lysosome. The macroautophagy is the lysosomal pathway responsible for the degradation of structures already located in the cytoplasm. Because the catabolic activity of lysosomes is used in this degradation, the structures to be degraded should be first separated from the cytoplasm (the lysosomal enzymes cannot be released directly to the cytoplasm). Phagosomes are the structures encharge of engulf the AGJ, isolating the AGJ from the cytoplasm, and with this action allowing the lysosomal fusion, degradation and subsequent recycling of the phagosome cargo and the phagosome membrane (Falk et al., 2012).

The preference for one degradative pathway over the other may be cell type dependent and within the same cell type the degradative pathway chosen might depend on the metabolic state of the cell.

Gollob et al., in 2006 showed that the M163V Cx40 mutant retain the ability to form plaques, these plaques are very similar to the ones form by the Cx40 WT. In the same paper they showed that the A96S mutant is able to form plaques but these are small in compared with WT and they also showed that the G38D mutant didn't show any plaque formation between cells. The assembly and breakdown of GJ hemi-channels features three key steps: insertion and correct folding of the Cx into the membranes, Cx oligomerization to generate hexameric hemi-channels, and their targeting to the plasma membrane (Oviedo-Orta et al., 2002). The Cx40 mutations could be modifying not only the electrical and permeability properties of the channels, but they could be also modifying the protein expression, any of the assembly steps and cause misfolding, oligomerization deficiencies, defects in their traffic to the membrane and/or plaque formation. In this study, the total protein level for all the mutants were test using the western blot technique. The protein level of the G38D and A96S mutants are similar to the WT protein level, but the M163V mutant presented a higher protein level than the WT. We also determined what organelle of the cells contained more Cx protein using immunofluorescence microscopy. The immunolabeling showed that all the mutations are able to form plaques, all three co-localize with the Golgi apparatus and the mutations G38D and A96S showed a high co-localization with the early endosome.

Experimental Design

We used western blot techniques to determine protein synthesis, and immunolabeling to determine the Cx40 mutants subcellular localization. We also used markers for Golgi and early endosome.

Western Blot analysis.- HeLa cells transfected homogenates were prepared 48 hrs after transfection with Cx40 mutants DNA. The protein concentration of the homogenates were determinated using the Bradford method (Bio-Rad). The proteins were separated by SDS-PAGE on 10 % polyacrylamide gels and blotts onto Immobilon transfer membranes (Millipore). The membranes were block using 3% milk in TBST for 1 hr at room temperature. After the blocking the membranes were washed 3 times, 5min each time, with 1x TBST. Cx40 was detected using a rabbit polyclonal anti-connexin 40 (Millipore) at 1: 500 dilution during 30 mins. After the incubation the membranes were washed 3 times, 5min each time, with 1x TBST. After the washes, the membranes were incubated for 1 hrs with secondary antibody Goat anti- rabbit (Santacruz) in a 1: 10,000 dilution. Immunoblots were developed with HyGLO Chemiluminescent HRP Antibdy Detection Reagent (Denville, Scientific) and exposure to a X-ray film. Band intensities were quantified using Image J program.

Immunolabeling analysis.- Coverslips with transfected HeLa cells were fixed in 3.7 % of formaldehyde prepared in 1x PBS (no Mg or Ca) for 15 mins. After 15 min de cells were wash several times with 1x PBS and after the wash, the cells were permeabilizd with .2 % of Triton 100 x for 4 mins. The cells were washed 3 times with 1x PBS and then blocked with 8% BSA prepared in 1x PBS for 1 hr. After 1 hr the cells were incubated with primary antibody for 1 hr at 37℃ in a humid chamber at 1:1000 dilution. For Golgi the antibody was abcam mouse

monoclonal (ab27043) and for endosome the antibody was abcam Anti-EEA1 mouse monoclonal (ab70521). After the incubation the coverslip were washed 3 times with 1x PBS for 5 min, each time. The cells were incubated with secondary antibody for 45 mins, at 37℃ in a humid chamber. The secondary antibody was Alexa Fluor 488 for both Golgi and endosome in a dilution of 1:10,000. After the incubation, the coverslips were washed 3 times, 5 mins each with 1x PBS. After the washes, the coverslips were incubated with anti Cx 40 rabbit antibody (Invitrogene) for 1 hr at 37℃ in a humid chamber in a 1:1000 dilution. After the incubation the coverslips were washed 3 times with 1x PBS for 5 min, each time. The cells were incubated with secondary antibody, in this case Texas red anti rabbit (Invitrogen) in a dilution of 1:10, 000, for 45 mins, at 37℃ in a humid chamber. After the incubation, the coverslips were washed 3 times, 5 mins each with 1x PBS. The coverslip were mount with Vectashield softmount plus DAPI (Vector, laboratories). Cells were studied using a Zeiss microscope (Carl Zeiss Meditec). Images were captures with a Zeiss AxioCam MRm camera usuing Zeiss AxioVision software.

Results

We tested the total protein level for all the mutants using western blot analysis. Our western blots showed that the total protein level for the two mutants, G38D and A96S are similar to that of WT (relatively intensity.- 0.11 A96S, 0.11 G38D and 0.10 WT)(Fig.IV-1). The protein level of the M163V mutants is higher than the WT (0.25 vs 0.10 relatively intensity). These results show that the mutations in the Cx40 are not affecting total protein production.

The assembly of GJ hemi-channels features three key steps: insertion and correct folding of Cx in to the membranes, Cx oligomerization to generate hexameric hemi-channels, and their targeting to the plasma membrane (Oviedo-Orta et al., 2002). So it is possible that the reduction in the amount of proteins is because the Cx is being destroyed during their synthesis or folding (we are not able to detect it by western blot) or their half life time is different and the rates of degradation is higher; either would make it so we used immunoflorescence microscopy to determine what organelle of the cells conteined more Cx protein. In the immunofluorescence microscopy for Cx40 WT, the Golgi body surround the nucleus, and the Cx forms a well-defined plaque and co-localizes with the Golgi body (Fig.IV-2).

The immunofluorescence labeling shows that in the case of the Cx40 M163V mutant the protein is still able to form plaques, but these are small and not very well defined. There is some co-localization with the Golgi and it appears that the Cx not only is at the plasma membrane in a plaque, but also is visible in the labeling that the Cx is also found in all the cell membrane and in high concentration at the cytoplasm (Fig.IV-2).

The Cx40 A96V mutant shows similar localization to that of the M163V. There is Cx at the plasma membrane, and it is able to form a small but well defined plaque. The mutant Cx co-localizes with the Golgi, the cytoplasm, and all around the plasma membrane (Fig.IV-2).

Microscopy shows that the Cx40 G38D mutant is also able to reach the plasma membrane and form plaques. The microscopy also shows that similar to the other mutants, the Cx co-localizes with the Golgi body and we could also detect within a plaque, and in the entirity of the cell membrane and cytoplasm (Fig.IV-2).

We also performed immunolabeling for the early endosome. The normal distribution of endosomes is around the nucleus and the connexin might co-localize with the endosome because it is part of the degradation pathway. The Cx40 WT follows this normal distribution (Fig.IV-3).

The Cx40 M163V mutant forms a well-defined plaque and co-localizes with the endosome. It appears that the proportion of mutant protein in the endosome is much higher that in WT (Fig.IV-3).

Both the A96S (Fig.IV-3) and G38D (Fig.IV-3) Cx40 mutants form plaques at the plasma membrane and co-localize with the endosome but the degree of co-localization is very high, suggesting that the amount of protein at the endosome is higher than in the WT and M163V mutant.

Discussion

Cx are co-translationally inserted into the ER, then trafficked through the Golgi body. While traveling through the secretory pathway, Cx oligomerize into hexameric connexons but it is not clear where this oligomerization takes place. Different studies suggest that oligomerization could occur in the ER, in ER-Golgi intermediate compartment, or in the trans-Golgi network (Su and Lau, 2012). In the Golgi the hemi-channels could be stored, sent back to the ER, or mainteained on the pathway to the cell membrane. The fact that the Cx40 WT and mutants co-localize with the Golgi (and in some form in the cytoplasm) is not surprising because this distribution is consistent with the biosynthetic pathway. An important observation is that while the co-localization of the Cx40 protein with the Golgi is normal, the apparent increase in the amount of mutant Cx in the Golgi is not. This excess of mutant protein in the Golgi could be caused by the protein causing folding problems due to the change in the amino acids, and these misfolded proteins could be sent back to the ER or to the cytoplasm for proteosome degradation.

Cells have evolved two degradation pathways, the endo/lysosomal and the phago/lysosomal pathway. During the endo/lysosomal pathway the annular gap junctions fuse with the endosome and then the lysosome. After entering the early endosome, endocyted proteins are trafficked further down the degradation pathway to the lysosome, to be recycled to the plasma membrane or be degradated by the lysosome (Leithe et al., 2012). Misfolded connexons could also be delivered directly from the Golgi to the endosome for degradation. Because of this process overlap the excess of protein at the endosome in the case of the Cx40 A96S and Cx40 G38D

mutants could be the results of misfolding, or an excess of protein at the Golgi resulting in direct transport from this organelle to the endosome for their degradation.

A high level of degradation of protein with mutations in the TM segments of membrane proteins is common. The TM segments of membrane proteins are commonly composed of hydrophobic α-helices (Caputo et al., 2003) and the change of amino acids to different hydrophobicities, size and/or ability to form hydrogen bonds could affect the folding and the insertion of the protein in the membrane. The mutations A96S and G38D could destabilize the protein, causing protein misfolding or a failure of membrane insertion. Either action could cause the retention of the protein at the Golgi, leading to the transport to the endosome for degradation of the protein. If the protein is transported to the membrane, either mutation could cause difficulties in the membrane insertion and send it to degradation.

It is known that not all the channels in a plaque are active. Bakauskas et al., 2000, calculated that in small plaques close to the critical size for function, only around 2% of the channels were active, and this fraction increase to 10-20% in plaques with diameters of 0.5 mm. Even when the immunolabeling of the mutants showed that the plaques are not as large as in the WT, we don't see a considerable difference in the gj. A possible explanation is that the number of active channels in plaques formed by the M163V and A96S mutants is very similar to that in the WT, even while the plaques are smaller. In the case of the G38D mutant the high single channel conductance (220 pS) could be balancing a reduction in the number of channels in the plaque. If, so, then even when the plaque could be smaller than WT plaques, the high unitary conductance of the G38D channels compensates for the reduction in the number of channels.

Figures and Tables

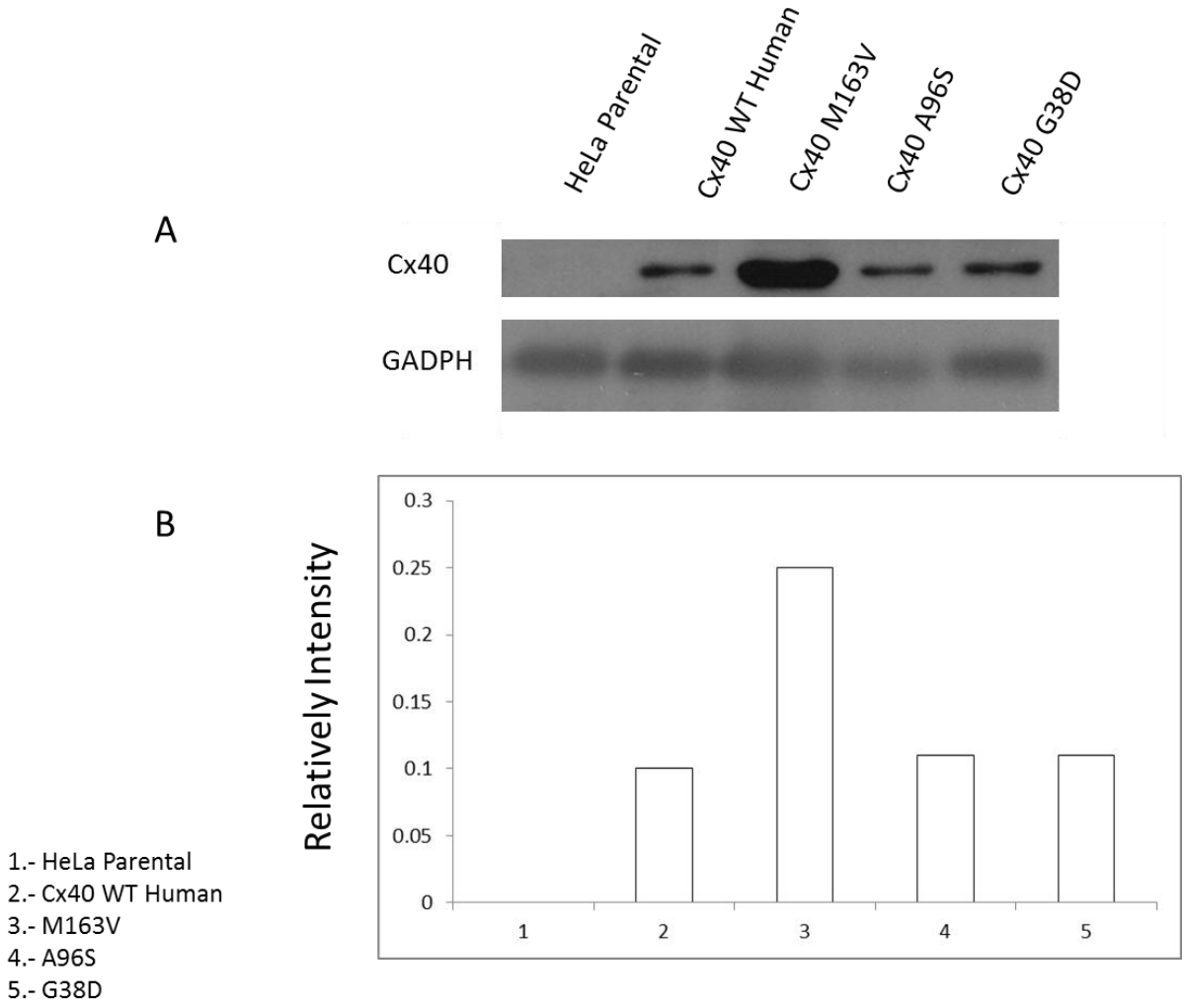

Fig.IV-1.- Western blot analysis of Cx40 protein. A, Protein extracts stained with Cx40 antibodies. B, Quantification of the mutants proteins extracts.

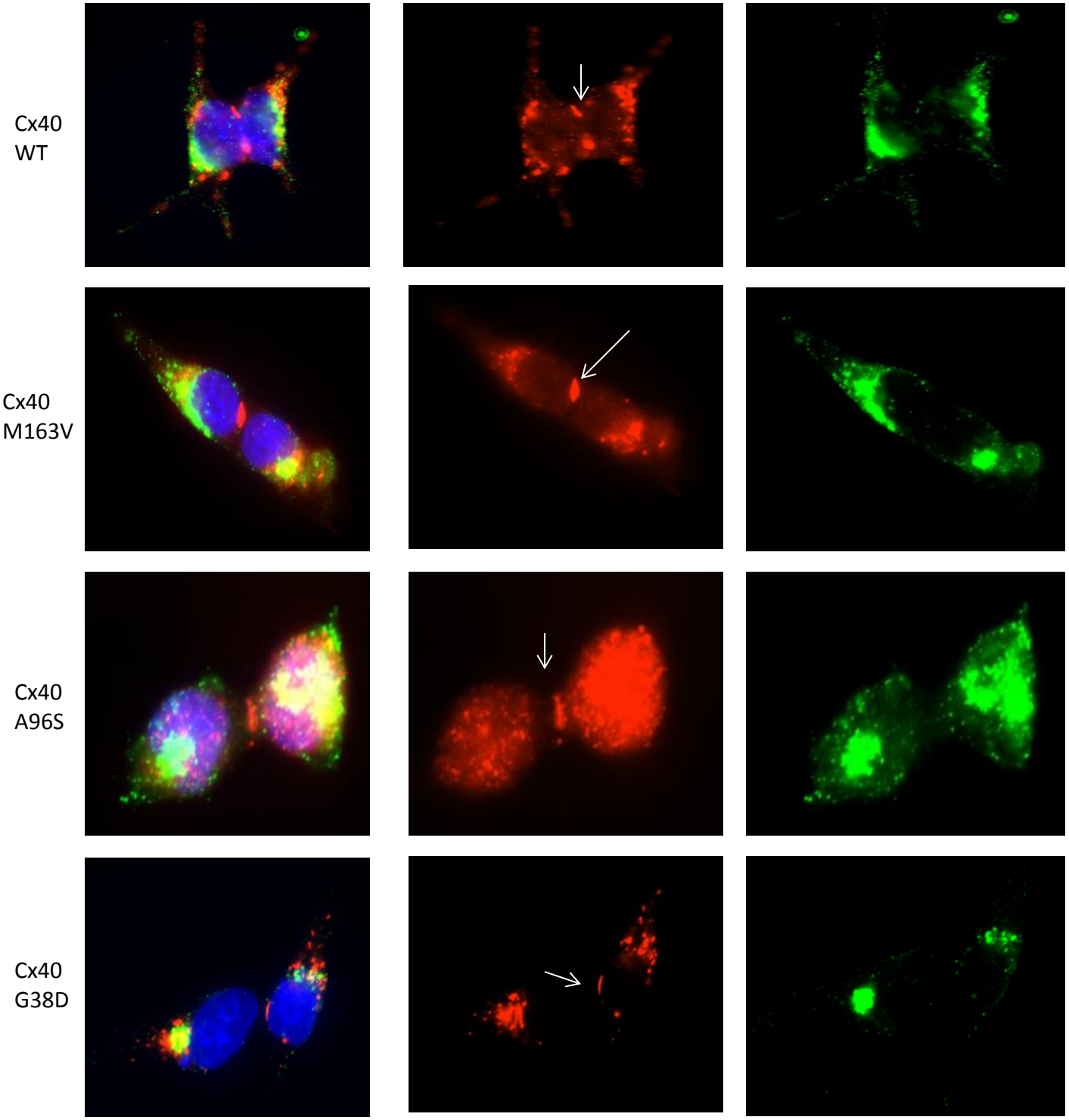

Fig.IV-2.- Double-label immunolocalization of Cx40 and Golgi. Cx40 WT, G38D, A96S and M163V mutants . Cx40 (red), Golgi (green), nucleus (blue).

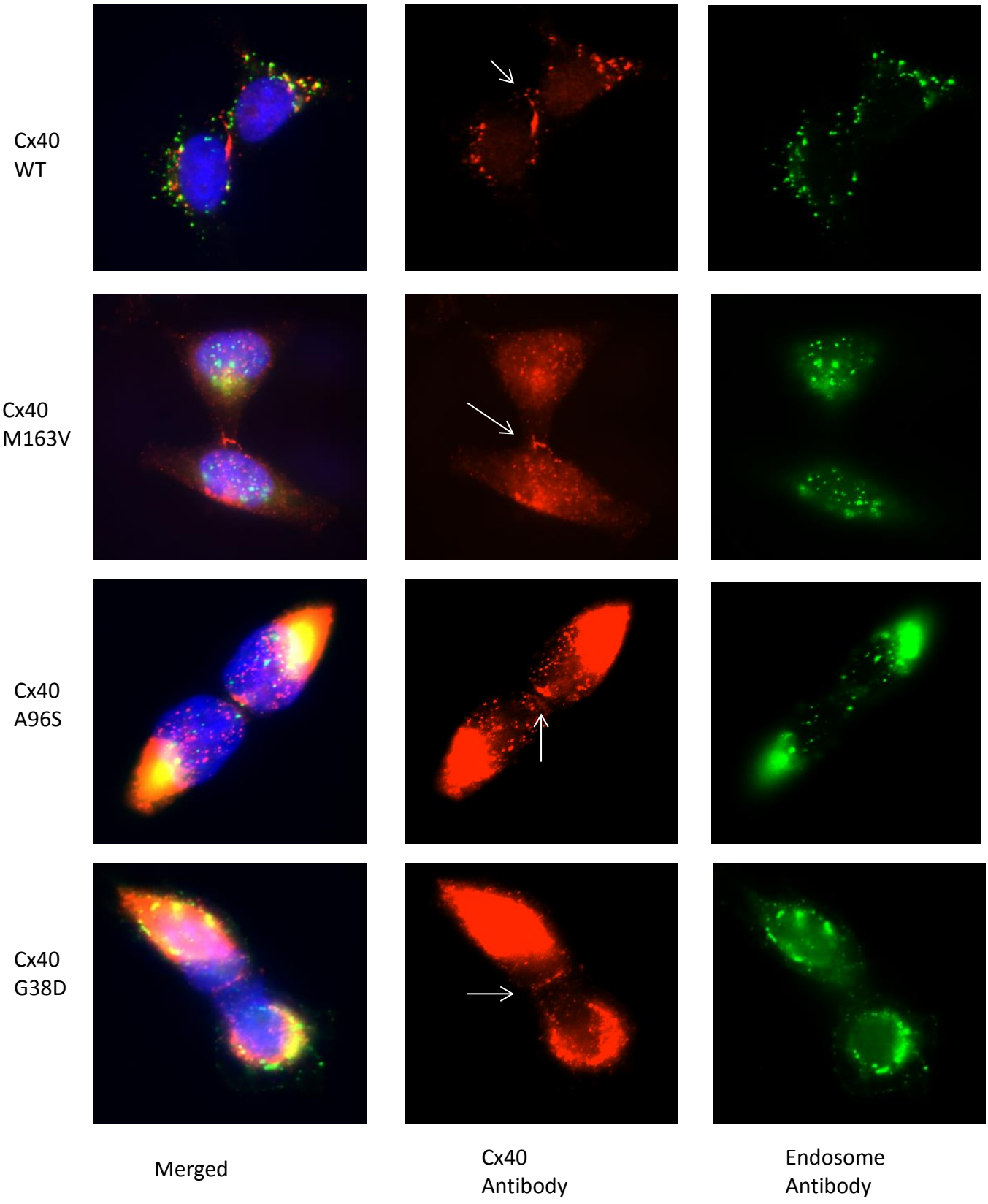

Fig.IV-3.- Double-label immunolocalization of Cx40 and endosome. Cx40 WT, G38D, A96S and M163V mutants. Cx40 (red), early endosome (green), nucleus (blue).

Chapter V

Relevance

AF occurs in conjunction with other cardiovascular disease such as hypertension, ischemic heart disease, valve disease or cardiac failure. However, in 20-50% of patients AF is not associated with any previously known disease (Brundel et al., 2002). Different studies point to two major mechanism involved in AF. The first possible mechanism is electrical remodeling, which consists of a change in the electrical properties of the atrium including prolongation of conduction, effective refractory period, and others. The second possible mechanism involved in AF is structural remodeling, which is an adaptative and maladaptive change in tissue and cellular architecture. Structural remodeling includes such changes as fibrosis, tissue de-differentiation, atrial dilatation and others (Korantzopoulos et al., 2007).

Efficient and well orchestrated spatial propagation of action potentials is achieved through organized cell-to-cell GJ coupling (Smyth et al., 2010). A major role of GJ in the myocardium is to enable rapid and coordinated electrical excitation, a prerequisite for normal rhythmic cardiac function, and also to facilitate intracellular exchange of small molecules (Saffitz and Kleber, 2004). Regulation of cell-to-cell communication by GJ involves changes that affect either the conductance states of a Cx protein, or processes that change the amount of Cx in the junctional plaque. Changes in the amount of protein in the plaque can occur through modification in trafficking, synthesis, or degradation (Saffitz and Kleber, 2004).

In order to have a better idea of how the Cx40 M163V, A96S and G38D mutations are related in AF, it is important to notice that the GJ do not exist in isolation and are part of larger macromolecular complexes and biological pathways (Veeraraghavan at al., 2014).

As shown above, we know that the permeability properties of the Cx40 mutants are different from that of the WT. Normal adult myocardial tissues show a preferred location of GJ at the longitudinal cell ends, and at smaller and less frequent junctions along the lateral borders. It has been demonstrated that cAMP (cyclic adenosine 3',5'-monophosphate) causes a significant increase in conduction velocity that appears to be attributable largely to enhanced expression of Cx (Darrow et al., 1996). Speculating that the increase of permeability of the Cx40 mutants holds true for cAMP, an increase of transfer between the cells could cause an increase of Cx expression. This increase of Cx expression could be causing an increase of the conduction velocity being an arrhythmia substrate. This increase in the permeability of cAMP could also be binding to and regulating the function of HCN channels.

cAMP is a ubiquitous intracellular second messenger that affects cell physiology by directly interacting with effector molecules that include cAMP-dependent protein kinases, cyclic nucleotide-gated ion channels, and hyperpolarization activated channels (Bedner et al., 2006). cAMP has a very short lifetime (1-60s) (Kasai and Petersen, 1994) and cAMP concentration in animal cells varies with the type and physiological state of the tissue. In general the cAMP concentration in tissue is in the range of 0.1 -1.0 μmole/Kg of wet weight (Beavo et al., 1974). It is generally accepted that cAMP increases the electrical cell-to-cell coupling in cardiac cells. This increase in coupling result from an increase in the probability of the channels being open due to the protein kinase A (PKA)-mediated phosphorylation of the Cxs, an augmentation of the synthesis of Cx protein or an increase in the number of channels with a higher conductance

(Matsumura et al., 2006). In the cardiac tissue cAMP also modulates the processes involved in excitation and contraction to increase the frequency of the SAN pacemaker, and the rate and extent of tension development during systole. At the same time, cAMP accelerates the rate of relaxation during diastole and reduces the overall duration of systole. Another very important function of the cAMP in the cardiac tissue is the modulation of the HCN channels. The HCN channel main function is the generation of the sinus rhytm and therefore heart rate control (Scicchitano et al., 2012). These channels are modulated by cAMP through a direct action on the channel itself, not by phosphorylations, as usually happens with other type of ion channels. The importance of the role of cAMP in the regulation of HCN channels could be found considering the inner characteristic of such proteins in controlling heart rate. Intracellular levels of cAMP increase in the SNA cells after a beta-adrenergic stimulation, while they decrease during vagal activation. These actions meadiate the role of the autonomic nervous system on the control of the heart rate. The permeability of Gj channels for cAMP is well demonstrated and could be very important in the control of physiological function at the cardiac tissue.

The Cx40 M163V, A96S and G38D mutations are mutations that may affect protein folding in two ways: (1) by impairing the folding process or decreasing the stability of the native state, both of which result in decreased steady state amounts of protein or (2) by promoting folding to stable, but nonfunctional conformations not removed by proteases which would aggregate or in other ways disturb cellular processes (Bross et al., 2011). The early endosome is defined as the first endocytic compartment to accept incoming cargo internalized from the PM (Gruenberg et al., 1989). Early endosomes are the primary sorting station in the endocytic pathway from which endocytosed molecules can be recycled back to the cell membrane or targeted for degradation in the lysosomes. We notice a high co-localization of the Cx40 mutants with the early endosome,

which could indicate that the Cx mutants are being removed from the membrane at a faster rate than that of WT. After proteins are sorted in the early endosome, those will be destroyed are moved to the lysosome for degradation. Excess of degradation or accumulation of misfolded protein could cause oxidative stress in the ER (Landau et al., 2013). Recent studies have demonstrated the implication of oxidative stress within the atrial tissue during AF suggesting a potential role in the remodeling phenomenon.

It is well documented that conduction though the atria is direction dependent, or anisotropic, with action potentials preferentially proceeding along the axial length of certain atrial muscle bundles (Kostin *et al.*, 2002). Two primary parameters determine the velocity at which an action potential can propagate through cardiac tissue. These parameters include the speed at which individual cells can depolarize and the resistance of the muscle fiber as a whole. The speed of depolarization depends on the kinetics of the membrane. This is related to the types, density, and localization of voltage gated ion channels found within the membrane of the cell (Kleber *et al.*, 2011). The muscle fiber resistance is proportional to its diameter, with increasing size providing a larger conduit for transmission, as well as cytoplasmic resistance and the conductance of cell-to-cell coupling via GJ. It has been observed that in AF patients Cx40 redistributes from polar to lateral cell membranes. The lateralization of the Cx could change the anisotropy and also could reduce the conduction velocity. Even when our results don't show a significant change in the total conductance of the junction, it could be that the lateralization of the channels is affecting the anisotropy and the conduction velocity, therefore contributing to the formation of an arrhythmogenic substrate for AF.

Chapter VI

References

- Abbaci M., Barbieri-Heyob M., Blondel W., Guillemin F., Didelon J. Advantages and limitations of commonly used methods to assay the molecular permeability of gap junctional intercellular communication. BioTechniques 45:33-62 (July 2008).

- Alías M, Ayuso-Tejedor S, Fernández-Recio J, Cativiela C, Sancho J.Helix propensities of conformationally restricted amino acids. Non-natural substitutes for helix breaking proline and helix forming alanine. Org Biomol Chem. 2010 Feb 21;8(4):788-92.

- Barnes TM. OPUS: a growing family of gap junction peoteins?. Trends Genet. 1994 Sep; 10(9):303-5.

- Beblo DA, Wang HZ, Beyer EC, Westphale EM, Veenstra RD.Unique conductance, gating, and selective permeability properties of gap junction channels formed by connexin40. Circ Res. 1995 Oct;77(4):813-22

- Bennett MV, Barrio LC, Bargiello TA, Spray DC, Hertzberg E, Sáez JC.Gap junctions: new tools, new answers, new questions. Neuron. 1991 Mar;6(3):305-20

- Berthoud VM, Minogue PJ, Laing JG, Beyer EC.Pathways for degradation of connexins and gap junctions. Cardiovasc Res. 2004 May 1;62(2):256-67.

- Beyer E.C., Paul D.L., Goodenough D.A. Connexin 43: a protein from rat heart homologous to a gap junction protein from the liver. J Cell Biol. 1987 Dec; 105(6 Pt 1): 2621-9.

- Beyer E.C., Lipkind G.M., Kyle J.W., Berthoud V.M. Structural organization of intracellular channelsII. Amino terminal domain of the connexins: sequence, functional roles, and structure. Biochim. Biophys. Acta 1818, 1823-1830. 2012

- Bird SD, Doevendans PA, van Rooijen MA, Brutel de la Riviere A, Hassink RJ, Passier R, Mummery CL. The human adult cardiomyocyte phenotype. Cardiovasc Res. 2003 May 1;58(2):423-34.

- Boassa D, Ambrosi C, Qiu F, Dahl G, Gaietta G, Sosinsky G. Pannexin1 channels contain a glycosylation site that targets the hexamer to the plasma membrane.J Biol Chem. 2007 Oct 26;282(43):31733-43.

- Bond SR, Naus CC. The pannexins: past and present.Front Physiol. 2014 Feb 19;5:58.

- Bross P, Corydon TJ, Andresen BS, Jørgensen MM, Bolund L, Gregersen N.Protein misfolding and degradation in genetic diseases. Hum Mutat. 1999;14(3):186-98.

- Brundel BJ, Henning RH, Kampinga HH, Van Gelder IC, Crijns HJ.Molecular mechanisms of remodeling in human atrial fibrillation. Cardiovasc Res. 2002 May;54(2):315-24. Review

- Bruzzone R, Hormuzdi SG, Barbe MT, Herb A, Monyer H. Pannexins, a family of gap junction proteins expressed in brain. Proc Natl Acad Sci U S A. 2003 Nov 11;100(23):13644-9.

- Bukauskas FF, Jordan K, Bukauskiene A, Bennett MV, Lampe PD, Laird DW, Verselis VK. Clustering of connexin 43-enhanced green fluorescent protein gap junction channels and functional coupling in living cells. Proc Natl Acad Sci U S A. 2000 Mar 14;97(6):2556-61.

- Caputo GA, London E.Cumulative effects of amino acid substitutions and hydrophobic mismatch upon the transmembrane stability and conformation of hydrophobic alpha-helices. Biochemistry. 2003 Mar 25;42(11):3275-85.

- Carmeliet E., Vereecke J. Cardiac cellular electrophysiology. Basic Science for the cardiologist.2002. Springer.

- Cruciani V, Mikalsen S.O. The vertebrate connexin family. Cell. Mol. Life. Sci. 2006. May; 63(10):1125-40.

- Dahl G, Werner R, Levine E, Rabadan-Diehl C. Mutational analysis of gap junction formation. Biophys J. 1991. Apr;62(1):172-80.

- Darrow BJ, Fast VG, Kléber AG, Beyer EC, Saffitz JE. Functional and structural assessment of intercellular communication. Increased conduction velocity and enhanced connexin expression in dibutyryl cAMP-treated cultured cardiac myocytes. Circ Res. 1996 Aug;79(2):174-83.

- Das Sarma J, Wang F, Koval M.Targeted gap junction protein constructs reveal connexin-specific differences in oligomerization. J Biol Chem. 2002 Jun 7;277(23):20911-8

- Davis LM1, Saffitz JE, Beyer EC.J Cardiovasc Electrophysiol. 1995 Feb;6(2):103-14. Modulation of connexin43 expression: effects on cellular coupling.

- Delmar M, Makita N. Cardiac connexins, mutations and arrhythmias. Curr Opin Cardiol. 2012 May;27(3):236-41.

- Dupont E, Ko Y, Rothery S, Coppen SR, Baghai M, Haw M, Severs NJ. The gap-junctional protein connexin40 is elevated in patients susceptible to postoperative atrial fibrillation. Circulation. 2001 Feb 13;103(6):842-9.

- de Diego C, Chen F, Xie Y, Pai RK, Slavin L, Parker J, Lamp ST, Qu Z, Weiss JN, Valderrábano M.Anisotropic conduction block and reentry in neonatal rat ventricular myocyte monolayers. Am J Physiol Heart Circ Physiol. 2011 Jan;300(1):H271-8

- Ek-Vitorin J.F., Burt J.M. Structural basis for the selective permeability of channels made of communicating junction proteins. Biochimica et Biophysica Acta 1828 (2013) 51-68.

- Elfgang C, Eckert R, Lichtenberg-Fraté H, Butterweck A, Traub O, Klein RA, Hülser DF, Willecke K.Specific permeability and selective formation of gap junction channels in connexin-transfected HeLa cells. J Cell Biol. 1995 May;129(3):805-17.

- Falk MM, Kells RM, Berthoud VM.Degradation of connexins and gap junctions. FEBS Lett. 2014 Apr 17;588(8):1221-9.

- Goldberg G.S., Valiunas V., Brink P.R. Selective permeabi8lity of gap junction channels. Biochim Biophys Acta. 2004 Mar 23;1662 (1-2):96-101.

- Goodenough D.A, Paul D.L. Gap Junctions, Cold Spring Harb. Perspect. Biol. 1, a002576.

-Gollob MH, Jones DL, Krahn AD, Danis L, Gong XQ, Shao Q, Liu X, Veinot JP, Tang AS, Stewart AF, Tesson F, Klein GJ, Yee R, Skanes AC, Guiraudon GM, Ebihara L, Bai D. Somatic mutations in the connexin 40 gene (GJA5) in atrial fibrillation. N Engl J Med. 2006 Jun 22;354(25):2677-88.

- Grant AO.Cardiac ion channels. Circ Arrhythm Electrophysiol. 2009 Apr;2(2):185-94

- Gray TM, Matthews BW.Structural analysis of the temperature-sensitive mutant of bacteriophage T4 lysozyme, glycine 156----aspartic acid. J Biol Chem. 1987 Dec 15;262(35):16858-64

- Gray RA., Jalife J., Panfilov A., Baxter WT., Cabo C., Davidenko JM., Pertson AM. Nonstationary vortexlike reentrant activity as mechanism of polymorphic ventricular tachycardia in the isolated rabbit heart. Circulation. 1995: 91:2454-2459.

- Groenewegen WA1, Firouzi M, Bezzina CR, Vliex S, van Langen IM, Sandkuijl L, Smits JP, Hulsbeek M, Rook MB, Jongsma HJ, Wilde AA. A cardiac sodium channel mutation cosegregates with a rare connexin40 genotype in familial atrial standstill.Circ Res. 2003 Jan 10;92(1):14-22.

-Gros DB, Jongsma HJ. Connexins in mammalian heart function. Bioessays. 1996 Sep;18(9):719-30. Review.

- Gruenberg J1, Griffiths G, Howell KE. Characterization of the early endosome and putative endocytic carrier vesicles in vivo and with an assay of vesicle fusion in vitro.J Cell Biol. 1989 Apr;108(4):1301-16.

- Guerrier A, Fonlupt P, Morand I, Rabilloud R, Audebet C, Krutovskikh V, Gros D, Rousset B, Munari-Silem Y.Gap junctions and cell polarity: connexin32 and connexin43 expressed in polarized thyroid epithelial cells assemble into separate gap junctions, which are located in distinct regions of the lateral plasma membrane domain. J Cell Sci. 1995 Jul;108 (Pt 7):2609-17

- Guida V, Ferese R, Rocchetti M, Bonetti M, Sarkozy A, Cecchetti S, Gelmetti V, Lpri F, Copetti M, Lamorte G, Cristina Digilio M, Marino B, Zaza A, den Hertog J, Dallapiccola B, De Luca A. A variant in the carboxyl-terminus of connexons 40 alters gap juncyions and increases risk for tetralogy of Fallot. Eur. J. Hum. Genet. 2013. Jan; 21(1):69-75

- Haubrich S, Schwarz H.J, Bukauskas F, Lichtenberg-Frate H, Traub O, Weingart R, Willecke K. Incompatibility od connexin 40 and 43 hemichannels in gap junctions between mammalian cells is determined by intracellular domains. Mol. Biol. Cell. 1996. Dec; 7(12):1995-2006.

- Hervé JC, Derangeon M. Gap-junction-mediated cell-to-cell communication.Cell Tissue Res. 2013 Apr;352(1):21-31.

- Hollingsworth SA, Karplus PA.A fresh look at the Ramachandran plot and the occurrence of standard structures in proteins. Biomol Concepts. 2010 Oct;1(3-4):271-283.

- Igarashi T, Finet JE, Takeuchi A, Fujino Y, Strom M, Greener ID, Rosenbaum DS, Donahue JK.Connexin gene transfer preserves conduction velocity and prevents atrial fibrillation. Circulation. 2012 Jan 17;125(2):216-25.

- Ikeda T., Czer L., Trento A., Hwang C., Ong JJC., Hough D., Fishbein MC., Mandel WJ., Karagueuzian HS., Chen PS. Induction of meandering functional reentrant wave front in isolated human atrial tissues. Circulation. 1997; 96:3013-3020.

- Imanaga I, Kameyama M, Irisawa H.Cell-to-cell diffusion of fluorescent dyes in paired ventricular cells. Am J Physiol. 1987 Jan;252(1 Pt 2):H223-32

- Johnson R, Hammer M, Sheridan J, Revel JP.Gap junction formation between reaggregated Novikoff hepatoma cells. Proc Natl Acad Sci U S A. 1974 Nov;71(11):4536-40.

- Kanaporis G, Brink PR, Valiunas V. Gap junction permeability: selectivity for anionic and cationic probes. Am J Physiol Cell Physiol. 2011 Mar;300(3):C600-9.

- Kemp BE, Pearson RB.Protein kinase recognition sequence motifs. Trends Biochem Sci. 1990 Sep;15(9):342-6.

- Kirchhoff S1, Nelles E, Hagendorff A, Krüger O, Traub O, Willecke K. Reduced cardiac conduction velocity and predisposition to arrhythmias in connexin40-deficient mice.Curr Biol. 1998 Feb 26;8(5):299-302.

-Kleber AG, Janse MJ, Fast VG. Normal and Abnormal Conduction in the Heart. 2011. USA: John Wiley and Sons, Inc.

- Kléber AG1, Rudy Y. Basic mechanisms of cardiac impulse propagation and associated arrhythmias. Physiol Rev. 2004 Apr;84(2):431-88.

- Korantzopoulos P, Kolettis TM, Galaris D, Goudevenos JA.The role of oxidative stress in the pathogenesis and perpetuation of atrial fibrillation. Int J Cardiol. 2007 Feb 7;115(2):135-43.

-Kostin S, Klein G, Szalay Z, Hein S, Bauer EP, Schaper J. Strcutural correlate of atrial fibrillation in human patients. Cardiovasc Res. 2002:54:361-379.

- Koval M.Sharing signals: connecting lung epithelial cells with gap junction channels. Am J Physiol Lung Cell Mol Physiol. 2002 Nov;283(5):L875-93

- Kreuzberg MM, Liebermann M, Segschneider S, Dobrowolski R, Dobrzynski H, Kaba R, Rowlinson G, Dupont E, Severs NJ, Willecke K. Human connexin31.9, unlike its orthologous protein connexin30.2 in the mouse, is not detectable in the human cardiac conduction system. J Mol Cell Cardiol. 2009 Apr;46(4):553-9.

-Kronengold J, Trexler EB, Bukauskas FF, Bagiello TA, Verselis VK. Pore-lining residues identified by single channel SCAM studies in Cx 46 hemichannels. Cell Commun Adhes. 2003. Jul-Dec; 10 (4-6): 193-9.

- Kwong KF1, Schuessler RB, Green KG, Laing JG, Beyer EC, Boineau JP, Saffitz JE. Differential expression of gap junction proteins in the canine sinus node.Circ Res. 1998 Mar 23;82(5):604-12.

- Landau G, Kodali VK, Malhotra JD, Kaufman RJ.Detection of oxidative damage in response to protein misfolding in the endoplasmic reticulum. Methods Enzymol. 2013;526:231-50

- Landesman Y, White TW, Starich TA, Shaw JE, Goodenough DA, Paul DL.Innexin-3 forms connexin-like intercellular channels. J Cell Sci. 1999 Jul;112 (Pt 14):2391-6.

- Laird DW.Life cycle of connexins in health and disease. Biochem J. 2006 Mar 15;394(Pt 3):527-43.

- Leithe E, Sirnes S, Fykerud T, Kjenseth A, Rivedal E.Endocytosis and post-endocytic sorting of connexins. Biochim Biophys Acta. 2012 Aug;1818(8):1870-9

- Lemoine MD, Duverger JE, Naud P, Chartier D, Qi XY, Comtois P, Fabritz L, Kirchhof P, Nattel S.Arrhythmogenic left atrial cellular electrophysiology in a murine genetic long QT syndrome model. Cardiovasc Res. 2011 Oct 1;92(1):67-74

- Li J. Alterations in cell adhesion proteins and cardiomyopathy.World J Cardiol. 2014 May 26;6(5):304-13.

- Li Z1, Migita K, Samways DS, Voigt MM, Egan TM.J Neurosci. 2004 Aug 18;24(33):7378-86. Gain and loss of channel function by alanine substitutions in the transmembrane segments of the rat ATP-gated P2X2 receptor.

- Lin X1, Gemel J, Glass A, Zemlin CW, Beyer EC, Veenstra RD. Connexin40 and connexin43 determine gating properties of atrial gap junction channels.J Mol Cell Cardiol. 2010 Jan;48(1):238-45.

- Lubkemier I, Machura K, Kurtz L, Neubauer B, Dobrowolski R, Schweda F, Wagner C, Willecke K, Kurtz A. The connexin 40 A96S mutation causes renin-dependent hypertension. J.Am. Soc. Nephrol.2011. Jun; 22(6): 1031-40.

- Lubkemier I, Andrie R, Lickfett L, Bosen F, Stockigt F, Dobrowolski R, Draffehn A.M, Fregeac J, Schultze J.L, Bukauskas FF, Schrickel J.W, Willecke K. The connexin 40 A96S mutation from a patient with atrial fibrillation causes decreased atrial conduction velocities and sustained episodes of induced atrial fibrillation in mice. J. Mol. Cell. Cardiol. 2013. Dec;65:19-32.

- Maeda S, Nakagawa S, Suga M, Yamashita E, Oshima A, Fujiyoshi Y, Tsukihara T. Structure of the connexin 26 gap junction channel at 3.5 A resolution. Nature. 2009. Apr 2; 458(7238):597-602.

- Makita N, Seki A, Sumitomo N, Chkourko H, Fukuhara S, Watanabe H, Shimizu W, Bezzina C.R, Hasdemir C, Mugishima H, Makiyama T, Baruteau A, Baron E, Horie M, Hagiwara N, Wilde A.A, Probst V, Le Marec H, Roden D.M, Mochizuki N, Schott J.J, Delmar M, A connexin 40 mutation associated with a malignant variant of progressive familial heart block type I. Cric. Arrhythm. Electrophysiol. 2012. Feb; 5(1):163-72.

- Moreno AP1, Laing JG, Beyer EC, Spray DC. Properties of gap junction channels formed of connexin 45 endogenously expressed in human hepatoma (SKHep1) cells.Am J Physiol. 1995 Feb;268(2 Pt 1):C356-65.

- Nielsen MS, Axelsen LN, Sorgen PL, Verma V, Delmar M, Holstein-Rathlou NH. Gap Junctions. Compr Physiol. 2012 Jul;2(3):1981-2035.

- Olesen MS, Nielsen MW, Haunsø S, Svendsen JH.Atrial fibrillation: the role of common and rare genetic variants. Eur J Hum Genet. 2014 Mar;22(3):297-306.

- Oshima A1, Matsuzawa T, Nishikawa K, Fujiyoshi Y. Oligomeric structure and functional characterization of Caenorhabditis elegans Innexin-6 gap junction protein. J Biol Chem. 2013 Apr 12;288(15):10513-21.

- Oviedo-Orta E, Errington RJ, Evans WH.Gap junction intercellular communication during lymphocyte transendothelial migration. Cell Biol Int. 2002;26(3):253-63.

- Padmanabhan S, York EJ, Stewart JM, Baldwin RL. Helix propensities of basic amino acids increase with the length of the side-chain. J Mol Biol. 1996 Apr 5;257(3):726-34.

- Panchin Y, Kelmanson I, Matz M, Lukyanov K, Usman N, Lukyanov S. A ubiquitous family of putative gap junction molecules. Curr Biol. 2000 Jun 29; 10(13):R473-4.

- Pantano S, Zonta F, Mammano F. A fully atomistic model of the Cx 32 connexon. PLoS One. 2008. Jul 2;3(7): e2614.

- Patel D, Gemel J, Xu Q, Simon AR, Lin X, Matiukas A, Beyer EC, Veenstra RD.Atrial fibrillation-associated connexin40 mutants make hemichannels and synergistically form gap junction channels with novel properties. FEBS Lett. 2014 Apr 17;588(8):1458-64

- Penuela S, Gehi R, Laird DW. The biochemistry and function of pannexin channels. Biochim Biophys Acta. 2013 Jan;1828(1):15-22.

- Peracchia C.Chemical gating of gap junction channels; roles of calcium, pH and calmodulin. Biochim Biophys Acta. 2004 Mar 23;1662(1-2):61-80

- Phelan P. Innexins: members of an evolutionarily conserved family of gap-junction proteins. Biochim Biophys Acta. 2005 Jun 10;1711(2):225-45.

- Phelan P, Bacon JP, Davies JA, Stebbings LA, Todman MG, Avery L, Baines RA, Barnes TM, Ford C, Hekimi S, Lee R, Shaw JE, Starich TA, Curtin KD, Sun YA, Wyman RJ. Innexins: a family of invertebrate gap-junction proteins. Trends Genet. 1998 Sep;14(9):348-9

- Rackauskas M., Verselis V.K., Bukauskas F.F. Permeability of homotypic and heterotypic gap junction channels formed of cardiac connexins mCx30.2, Cx40, Cx43 and Cx45. Am J Physiol Heart Circ Physiol 293:H1729-H1736, 2007.

- Rohl CA, Fiori W, Baldwin RL.Alanine is helix-stabilizing in both template-nucleated and standard peptide helices. Proc Natl Acad Sci U S A. 1999 Mar 30;96(7):3682-7.

- Rohr S. Role pf gap junctions in the propagation of the cardiac action potential. Cardiovascular Research 62 (2004) 309-322.

- Saffitz JE, Kanter HL, Green KG, Tolley TK, Beyer EC.Tissue-specific determinants of anisotropic conduction velocity in canine atrial and ventricular myocardium. Circ Res. 1994 Jun;74(6):1065-70.

- Saffitz JE, Kléber AG. Effects of mechanical forces and mediators of hypertrophy on remodeling of gap junctions in the heart. Circ Res. 2004 Mar 19;94(5):585-91.

- Schmitt N, Grunnet M, Olesen SP.Cardiac potassium channel subtypes: new roles in repolarization and arrhythmia. Physiol Rev. 2014 Apr;94(2):609-53.

- Segretain D, Falk MM. Regulation of connexin biosynthesis, assembly, gap junction formation, and removal.Biochim Biophys Acta. 2004 Mar 23;1662(1-2):3-21.

- Severs NJ, Coppen SR, Dupont E, Yeh HI, Ko YS, Matsushita T.Gap junction alterations in human cardiac disease. Cardiovasc Res. 2004 May 1;62(2):368-77.

- Severs NJ, Bruce AF, Dupont E, Rothery S.Remodelling of gap junctions and connexin expression in diseased myocardium. Cardiovasc Res. 2008 Oct 1;80(1):9-19

- Sherwood L. Human Physiology, From Cells to Systems. 2008. Cengage Learning. 7th edition.

- Skerrett I.M., Aronowitz J, Shin J.H., Cymes G, Kasperek E, Cao F.L, Nicholson B.J. Identification of amino acid residues lining the pore of a gap junction channel. J. Cell. Biol. 2002. Oct 28; 159(2): 349-60.

- Smyth JW, Hong TT, Gao D, Vogan JM, Jensen BC, Fong TS, Simpson PC, Stainier DY, Chi NC, Shaw RM.Limited forward trafficking of connexin 43 reduces cell-cell coupling in stressed human and mouse myocardium. J Clin Invest. 2010 Jan;120(1):266-79.

- Stebbings LA, Todman MG, Phelan P, Bacon JP, Davies JA. Two Drosophila innexins are expressed in overlapping domains and cooperate to form gap-junction channels.Mol Biol Cell. 2000 Jul;11(7):2459-70.

- Su V, Lau AF.Ubiquitination, intracellular trafficking, and degradation of connexins. Arch Biochem Biophys. 2012 Aug 1;524(1):16-22.

-Sun Y, Yang Y.Q, Gong X.Q, Wang X.H, Li R.G, Tan H.W, Liu X, Fang W.Y, Bai D. Novel germline GJA/connexin 40 mutations associated with lone atrial fibrillation impair gap junctional intercellular communication. Hum. Mutat. 2013. Apr; 34(4):603-9.

- Sun Y, Tong X, Chen H, Huang T, Shao Q, Huang W, Laird D.W, Bai D. An atrial-fibrillation-linked connexin 40 mutant is retained in the endoplasmic reticulum and impairs the function of atrial gap-junction channels. Dis. Model. Mech. 2014. May; 7(5): 561-9.

- Thévenin AF, Kowal TJ, Fong JT, Kells RM, Fisher CG, Falk MM.Proteins and mechanisms regulating gap-junction assembly, internalization, and degradation. Physiology (Bethesda). 2013 Mar;28(2):93-116

-Thévenin AF, Kowal TJ, Fong JT, Kells RM, Fisher CG, Falk MM.Proteins and mechanisms regulating gap-junction assembly, internalization and degradation. Physiology (Bethesda). 2013 Mar;28(2):93-116.

- Tucker NR, Ellinor PT.Emerging directions in the genetics of atrial fibrillation. Circ Res. 2014 Apr 25;114(9):1469-82.

- Unger VM, Kumar NM, Gilula NB, Yeager M. Three-dimensional structure of a recombinant gap junction membrane channel. Science. 1999 Feb 19;283(5405):1176-80.

- Valderrábano M.Influence of anisotropic conduction properties in the propagation of the cardiac action potential. Prog Biophys Mol Biol. 2007 May-Jun;94(1-2):144-68.

-Valiunas V, Polosina YY, Miller H, Potapova IA, Valiuniene L, Doronin S, Mathias RT, Robinson RB, Rosen MR, Cohen IS, Brink PR. Connexin-specific cell-to-cell transfer of short interfering RNA by gap junctions. J Physiol. 2005 Oct 15;568(Pt 2):459-68. Epub 2005 Jul 21.

- Valiunas V, Beyer EC, Brink PR.Cardiac gap junction channels show quantitative differences in selectivity. Circ Res. 2002 Jul 26;91(2):104-11.

- Van Kempen MJ, Vermeulen JL, Moorman AF, Gros D, Paul DL, Lamers WH.Developmental changes of connexin40 and connexin43 mRNA distribution patterns in the rat heart. Cardiovasc Res. 1996 Nov;32(5):886-900

- van der Velden HM1, Ausma J, Rook MB, Hellemons AJ, van Veen TA, Allessie MA, Jongsma HJ. Gap junctional remodeling in relation to stabilization of atrial fibrillation in the goat.Cardiovasc Res. 2000 Jun;46(3):476-86.

- van Rijen HV, van Veen TA, Hermans MM, Jongsma HJ.Human connexin40 gap junction channels are modulated by cAMP. Cardiovasc Res. 2000 Mar;45(4):941-51

- van Veen AA, van Rijen HV, Opthof T. Cardiac gap junction channels: modulation of expression and channel properties. Cardiovasc Res. 2001 Aug 1;51(2):217-29.

- Veeraraghavan R, Gourdie RG, Poelzing S.Mechanisms of cardiac conduction: a history of revisions. Am J Physiol Heart Circ Physiol. 2014 Mar 1;306(5):H619-27

- Veenstra RD, Wang HZ, Westphale EM, Beyer EC.Multiple connexins confer distinct regulatory and conductance properties of gap junctions in developing heart. Circ Res. 1992 Nov;71(5):1277-83.

- Veenstra R.D., Wang Hong-Zang, Beblo D.A., Chilton M.G., Harris A.L., Beyer E.C. Brink P.R. Selectivity of connexin-specific gap junctions does not correlate with channel conductance. Circulation Research 1995; 77:1156-1165.

- Voges D, Zwickl P, Baumeister W.The 26S proteasome: a molecular machine designed for controlled proteolysis. Annu Rev Biochem. 1999;68:1015-68.

- Vozzi C, Dupont E, Coppen SR, Yeh HI, Severs NJ.Chamber-related differences in connexin expression in the human heart. J Mol Cell Cardiol. 1999 May;31(5):991-1003

- Wakili R, Clauss S, Schmidt V, Ulbrich M, Hahnefeld A, Schüssler F, Siebermair J, Kääb S, Estner HL.Impact of real-time contact force and impedance measurement in pulmonary vein isolation procedures for treatment of atrial fibrillation. Clin Res Cardiol. 2014 Feb;103(2):97-106.

- Welsh MJ, Smith AE. Cell. 1993 Jul 2;73(7):1251-4. Molecular mechanisms of CFTR chloride channel dysfunction in cystic fibrosis.

- Wilhelm M1, Kirste W, Kuly S, Amann K, Neuhuber W, Weyand M, Daniel WG, Garlichs C. Atrial distribution of connexin 40 and 43 in patients with intermittent, persistent, and postoperative atrial fibrillation.Heart Lung Circ. 2006 Feb;15(1):30-7. Epub 2005 Aug 25.

- Woods CE, Olgin J.Atrial fibrillation therapy now and in the future: drugs, biologicals, and ablation. Circ Res. 2014 Apr 25;114(9):1532-46.

- Wu CL, Shih MF, Lai JS, Yang HT, Turner GC, Chen L, Chiang AS. Heterotypic gap junctions between two neurons in the drosophila brain are critical for memory. Curr Biol. 2011 May 24;21(10):848-54

- Yang Y.Q, Zhang X.L, Wang X.H, Tan H.W, Shi H.F, Jiang W.F, Liu X. Connexin 40 nonsense mutation in familial atrial fibrillation. Int. J. Mol. Med. 2010. Oct; 26(4): 605-10.

- Yang Y.Q., Liu X, Zhang X.L., Wang X.H, Tan H.W, Shi W.F, Fang W.Y. Novel connexin 40 missese mutations in patients with familial atrial fibrillation. Europace. 2010. Oct; 12(10):1421-7.

- Zonta F, Polles G, Zanotti G, Mammano F.Permeation pathway of homomeric connexin 26 and connexin 30 channels investigated by molecular dynamics. J Biomol Struct Dyn. 2012;29(5):985-98